

FINAL REPORT

Bioaugmentation with Vaults: Novel In Situ Remediation Strategy for Transformation of Perfluoroalkyl Compounds

SERDP Project ER-2422

JANUARY 2016

Shaily Mahendra, PhD
Leonard H. Rome, PhD
Valerie A. Kickhoefer, PhD
Meng Wang, MS
University of California, Los Angeles

Distribution Statement A

This document has been cleared for public release



Page Intentionally Left Blank

This report was prepared under contract to the Department of Defense Strategic Environmental Research and Development Program (SERDP). The publication of this report does not indicate endorsement by the Department of Defense, nor should the contents be construed as reflecting the official policy or position of the Department of Defense. Reference herein to any specific commercial product, process, or service by trade name, trademark, manufacturer, or otherwise, does not necessarily constitute or imply its endorsement, recommendation, or favoring by the Department of Defense.

Page Intentionally Left Blank

REPORT DOCUMENTATION PAGE

Form Approved
OMB No. 0704-0188

The public reporting burden for this collection of information is estimated to average 1 hour per response, including the time for reviewing instructions, searching existing data sources, gathering and maintaining the data needed, and completing and reviewing the collection of information. Send comments regarding this burden estimate or any other aspect of this collection of information, including suggestions for reducing the burden, to Department of Defense, Washington Headquarters Services, Directorate for Information Operations and Reports (0704-0188), 1215 Jefferson Davis Highway, Suite 1204, Arlington, VA 22202-4302. Respondents should be aware that notwithstanding any other provision of law, no person shall be subject to any penalty for failing to comply with a collection of information if it does not display a currently valid OMB control number.
PLEASE DO NOT RETURN YOUR FORM TO THE ABOVE ADDRESS.

1. REPORT DATE (DD-MM-YYYY) 15/01/2016		2. REPORT TYPE Technical		3. DATES COVERED (From - To) 20/08/2014 - 20/08/2016	
4. TITLE AND SUBTITLE Bioaugmentation with Vaults: Novel in situ Remediation Strategy for Transformation of Perfluoroalkyl Compounds				5a. CONTRACT NUMBER W912HQ-14-C-0052	
				5b. GRANT NUMBER	
				5c. PROGRAM ELEMENT NUMBER	
6. AUTHOR(S) Mahendra, Shaily Rome, Leonard H. Kickhoefer, Valerie A. Wang, Meng				5d. PROJECT NUMBER ER-2422	
				5e. TASK NUMBER	
				5f. WORK UNIT NUMBER	
7. PERFORMING ORGANIZATION NAME(S) AND ADDRESS(ES) University of California, Los Angeles Department of Civil and Environmental Engineering 5732 Boelter Hall, Los Angeles, CA 90095-1593				8. PERFORMING ORGANIZATION REPORT NUMBER	
9. SPONSORING/MONITORING AGENCY NAME(S) AND ADDRESS(ES) SERDP				10. SPONSOR/MONITOR'S ACRONYM(S)	
				11. SPONSOR/MONITOR'S REPORT NUMBER(S)	
12. DISTRIBUTION/AVAILABILITY STATEMENT Unlimited					
13. SUPPLEMENTARY NOTES					
14. ABSTRACT The objective of this research was to develop an innovative in situ bioremediation technology using vault nanoparticles that will facilitate the degradation of poly- and perfluoroalkyl compounds (PFCs), and potentially other water contaminants, without the need for repeated bioaugmentation with active cultures or stimulation with nutrients. We designed a single-step method for encapsulating lgnln peroxidases (LiP), manganese peroxidases (MnP), and laccases into vaults. Vault-packaged enzymes were stable across a broader range of temperatures and pH, and in PFC-contaminated groundwater. Since vaults occur in nature, their application is unlikely to cause any risk for public health as well as the environment.					
15. SUBJECT TERMS					
16. SECURITY CLASSIFICATION OF:			17. LIMITATION OF ABSTRACT	18. NUMBER OF PAGES	19a. NAME OF RESPONSIBLE PERSON
a. REPORT	b. ABSTRACT	c. THIS PAGE			Shaily Mahendra
			SAR		19b. TELEPHONE NUMBER (Include area code) 310-794-9850

Page Intentionally Left Blank

Table of Contents

ABSTRACT	1
BACKGROUND	3
Poly- and perfluoroalkyl compounds (PFCs)	3
Vault Nanoparticles	5
Ligninolytic Enzymes	6
MATERIALS AND METHODS	7
Enzyme Activity Assay	7
Heterologous Expression of INT Fused Ligninolytic Enzymes, and Packaging of Recombinant Enzymes into Recombinant Vaults	7
<i>Cloning of Ligninolytic Enzymes Coding Sequences</i>	8
<i>Expression of INT Fused Ligninolytic Enzymes</i>	10
<i>Packaging and Characterization of INT-Fused Enzymes in Vault Nanoparticles</i>	11
Evaluation of the Stability and Performance of Vault-Packaged Enzymes	11
<i>Thermal Stability</i>	11
<i>Structural Stability of Empty Vault Nanoparticles</i>	12
<i>Performance Under Various pH</i>	12
Degradation of Perfluorooctanoic Acid.....	12
<i>Degradation of Perfluorooctanoic Acid by Fungal Cultures</i>	12
<i>Degradation of Perfluorooctanoic Acid by In vitro Enzymes</i>	13
RESULTS AND DISCUSSION	14
Cloning of Ligninolytic Enzymes Coding Genes	14
Heterologous Expression and Activity Test of INT-Fused Ligninolytic Enzymes	15
<i>Expression of nsLiP-INT and nsMnP-INT</i>	15
<i>Expression of sMnP-INT</i>	15
<i>Expression of Laccase-INT</i>	17
<i>Activity Test of INT-Fused Ligninolytic Enzymes</i>	18
Packaging of sMnP-INT in Vault Nanoparticles.....	19
Performance of Vaults Packaged with sMnP-INT	21
<i>Kinetics of sMnP-INT and Vault-Packaged sMnP-INT</i>	21
<i>Thermal Stability of Vault-Packaged sMnP-INT</i>	23
<i>Structural Stability of Vault Nanoparticles</i>	24
<i>Activity of Vault-Packaged sMnP-INT at Various pH</i>	27
Degradation of Perfluorooctanoic Acid.....	28
<i>Degradation of Perfluorooctanoic Acid by Fungal Cultures</i>	28
<i>Degradation of Perfluorooctanoic Acid by In vitro Enzymes</i>	29
CONCLUSIONS AND IMPLICATIONS FOR FUTURE RESEARCH	33
REFERENCES	37
APPENDICES	44

List of Figures

Figure 1. Vault Nanoparticles	6
Figure 2. Schematic of Vault Packaging.....	9
Figure 3. Western Blot Analysis of Lysate of Baculovirus Infected Sf9 Cells	16
Figure 4. Western Blot Analysis of Cell Lysate and Culture Supernatant of sMnP-INT Baculovirus Infected Sf9 Cells	17
Figure 5. ABTS Oxidation Test on Methanol Plate.....	18
Figure 6. Peroxidase Activity Test of sMnP-INT.....	19
Figure 7. Packaging of sMnP-INT into Vault Nanoparticles	20
Figure 8. ABTS Diffusion Analysis.....	22
Figure 9. Enhanced Thermal Stability of Vault-packaged sMnP-INT	25
Figure 10. Enzyme Activity Decay Modeling	26
Figure 11. TEM Images of Vault Nanoparticles Incubated at Different Conditions.....	27
Figure 12. Relative Activity of sMnP-INT-vault and sMnP-INT at Various pH Normalized to Their Activities at pH 4.01.....	28
Figure 13. Transformation of PFOA Exposed to <i>P. chrysosporium</i> in Nutrient-Rich and -Poor Medium.....	30
Figure 14. Transformation of PFOA Exposed to <i>T. versicolor</i> in Nutrient-Rich and -Poor Medium.....	31
Figure 15. Transformation of PFOA Exposed to Vault-Packaged sMnP-INT, Unpackaged sMnP- INT and nMnP	32

List of Tables

Table 1. Experimental Conditions for Vaults Structural Stability Tests	12
Table 2. Experimental Conditions for Fungi Exposed to PFOA	13
Table 3. Experimental Conditions for PFOA Exposed to Fungi-Produced Enzymes	14
Table 4. Experimental Conditions for PFOA Exposed to Three Types of MnP	14
Table 5. Km Values of sMnP-INT, sMnP-INT-vault, and naturally-produced MnP from the fungus <i>Phanerochaete chrysosporium</i>	22
Table 6. Values of k_1 , k_2 and α for sMnP-INT, sMnP-INT-vault, and Naturally-produced MnP from the fungus <i>Phanerochaete chrysosporium</i>	26

Abstract

Objectives and Rationale

The overall goal of this research was to develop an innovative *in situ* bioremediation technology using vault nanoparticles packaged with biodegradative enzymes that will facilitate the degradation of poly- and perfluoroalkyl compounds (PFCs), and potentially other water contaminants.

The use of molecular-engineered enzyme catalysts for removing compounds of emerging concern is an innovative and sustainable approach for environmental restoration. Photochemical and electrochemical oxidation processes tend to be energy- and cost-intensive, whereas biological treatment using microbial whole cells is constrained by geochemical characteristics and by the concerns of biofouling, potentially releasing pathogens, and affecting microbial ecology of the natural and engineered systems.

This research was proposed to develop a single-step method for encapsulating active enzymes in recombinant vaults, which are naturally synthesized, hollow ribonucleoprotein particles. Lignin peroxidase (LiP), manganese peroxidase (MnP), and laccase enzymes are produced by wood-rotting fungi to digest lignin, which is a complex plant polymer. Several studies have demonstrated that wood-rotting fungi and their extracellular enzymes can degrade certain PFCs. Biodegradation using fungal whole cells relies on the culture growth, which is highly dependent on the biogeochemical conditions such as pH, temperature, nutrient status, and oxygen levels at contaminated sites. Using their extracellular enzymes directly is a promising alternative approach, because *in vitro* enzymes tend to be more efficient, and less constrained by the requirements for microbial growth. The limited stability of free enzymes in natural environments, however, restricts their implementation. We hypothesized that packaging ligninolytic enzymes, such as peroxidases and laccases, into vault nanoparticles for remediation of PFCs will eliminate the reliance on fungal growth and repeated injections of purified enzymes by enhancing *in situ* stability of multiple enzymes simultaneously.

Technical Approach

Prior to packaging fungal peroxidases and laccase into vault particles, the enzymes were modified with an INT targeting domain, which has strong affinity to the vault interior. Recombinant LiP-INT and MnP-INT were produced in insect Sf9 cell lines using a Bac-to-Bac expression system; and INT-attached laccase was produced in yeast *Pichia pastoris* under a methanol-inducing promoter. Prior to encapsulation, the activities of recombinant enzymes were tested to screen the active enzymes for subsequent tests. Next, we evaluated if active INT-modified enzymes could be packaged and retain their enzyme activities inside vault particles. Upon confirmation of enzymatic activity of INT-attached enzymes and vault-packaged enzymes, their capacity to transform perfluorooctanoic acid (PFOA) was determined. Reactions were conducted in 1 mL vials containing 1-10 mg/L PFOA, reaction

buffer, different types of enzymes and hydrogen peroxide, if necessary. Transformation of PFOA using whole cells of two wood-degrading fungi, *Phanerochaete chrysosporium*, which produces LiP and MnP, and *Trametes versicolor*, which produces laccase, was also performed. All samples were monitored for PFOA concentrations and the potential metabolite concentrations. Finally, the stability of fungal enzymes, INT-modified enzymes, and vault-packaged enzymes were compared by measuring enzymatic activities over extended periods of time at different temperatures and in PFC-contaminated groundwater samples.

Results

INT-modified LiP and MnP were heterologously expressed in Sf9 insect cell lines intracellularly as nsLiP-INT and nsMnP-INT through Bac-to-Bac expression systems. Both expressions were confirmed by Western blots using anti-INT antibodies. Cell lysates containing nsLiP-INT or nsMnP-INT did not show significant peroxidase activities, suggesting that signal peptide processing contributes to correct folding of peroxidases and is likely required to activate these enzymes.

INT-fused MnP was also expressed extracellularly in Sf9 cell lines as sMnP-INT using its natural signal sequence. Vault-packaged sMnP-INT enzymes were isolated *via* ultracentrifuging mixtures of empty vault nanoparticles and culture supernatants containing sMnP-INT molecules. The integrity of vaults packaged with sMnP-INT was confirmed with negative stain transmission electron microscopy. Both free sMnP-INT and vault-packaged sMnP-INT showed manganese(II) ion dependent activity identical to that of MnP produced by *P. chrysosporium*, revealing that sMnP-INT maintained its activity when packaged inside vaults. Thermal stability of packaged sMnP-INT was compared with that of free sMnP-INT and MnP from *P. chrysosporium*, and it was found that vaults packaged sMnP-INT underwent slower deactivation at 20°C, 30°C and 40°C. Further deactivation kinetics study showed the enhanced thermal stability was due to the constraint from the vault shell, which prevents the enzymes from conformational changes. Empty vault nanoparticles showed excellent structural stability in the presence of PFCs in a phosphate buffer. Intact vault structure was maintained for at least 32 days. Additionally, to understand the performance of vault-packaged sMnP-INT under more realistic conditions, we examined the activity of sMnP-INT-vault and sMnP-INT under pH values ranging from 2.5 to 6.0 because MnP exhibits optimum activity at pH 4.0. The data showed sMnP-INT packaged in vaults had better activity at weakly acidic pH (5.0-6.0), indicating that vault nanoparticles were able to maintain the activity of packaged sMnP-INT against large pH changes.

INT-fused laccase was expressed as a secreted enzyme in *Pichia pastoris* under methanol inducing conditions, and was demonstrated to be active on methanol containing agar. However, the activity of recombinant laccase was below the detection limit when grown in liquid medium. Thus, it was not packaged into vaults in the duration of the 1-year project.

Neither fungal whole cells of *P. chrysosporium* and *T. versicolor*, nor free enzymes including LiP, MnP, and laccase could transform PFOA under the limited experimental conditions used in this study. Free and vault packaged sMnP-INT enzymes were also tested, but no statistically significant transformation was observed. Possible reasons for little to no PFOA transformation include short incubation times, low enzyme concentrations, lack of mediators, and analytical limitations.

Benefits and SERDP Relevance

Groundwater at many DoD sites has been contaminated with not only perfluoroalkyl compounds but also many other chemicals of ecological and public health concerns, such as estrogenic compounds, energetic compounds like RDX, and polybrominated diphenyl ethers (PBDEs). This limited scope did not yet confirm biodegradation of perfluoroalkyl compounds in contaminated groundwater, but produced extremely promising results using a novel nanobiotechnology. Thus, it will support SERDP's mission to reduce the DoD's liabilities by developing innovative and sustainable vault-based technologies for expedited site cleanup and closure by *in situ* remediation of RDX and PBDEs and other contaminant mixtures in groundwater.

Vault packaged enzymes are more stable under diverse biogeochemical conditions and long-lived than free enzymes, and eliminate the need for repeated bioaugmentation with active cultures or stimulation with nutrients. The integration of vault particles with MnP serves as the foundation for implementing vault-based *in situ* bioremediation with the potential to lead to more customized enzyme catalyzed solutions for waste treatment and contaminated sites. The vaults can be custom-produced on a large scale, and applied in various *in situ* bioaugmentation approaches to concurrently remove multiple contaminants. Since vaults occur in nature, and have been isolated from many eukaryotes including humans, their application is unlikely to cause any risk for human health as well as the environment. Thus, the design of stable vehicles for safely packaging enzymes that can be integrated with current groundwater treatment technologies would result in a fundamentally transformative approach for the degradation of emerging water contaminants.

Background

Poly- and perfluoroalkyl compounds (PFCs)

Poly- and perfluoroalkyl compounds (PFCs) are extremely stable chemicals that contain a 4-8 carbon chain bonded to fluorine.[1] Because of fluorine's high electron affinity and high electronegativity, carbon-fluorine bonds are strong covalent bonds and have high bond energy, which result in the excessive stability of PFCs. Due to their unique properties, PFCs have been widely used in industrial, commercial, and military products, including surfactant, non-stick coating, sealants, insulation, and aqueous fire-fighting foams (AFFFs).[2-5] Since AFFFs are highly stable and resistant to most biodegradation, and have

been extensively used to extinguish hydrocarbon fires at DoD sites and other industrial facilities for decades, these sites are likely to be contaminated by high concentrations of PFCs in soil and groundwater.[6, 7] Particularly, perfluorooctanoic acid (PFOA), in which all carbon-hydrogen bonds are substituted by carbon-fluorine bonds, is one of the most persistent PFCs in the environment.[8-10] Several research indicates that PFCs, especially PFOA, are development toxicants,[11] probable carcinogens, immune system toxicants, and bioaccumulative in human and wildlife.[8, 12-15] PFOA may be directly released from commercial products, such as AFFFs or result from transformation of polyfluoroalkyl compounds in the environment, such as 8:2 fluorotelomer alcohol (FTOH).

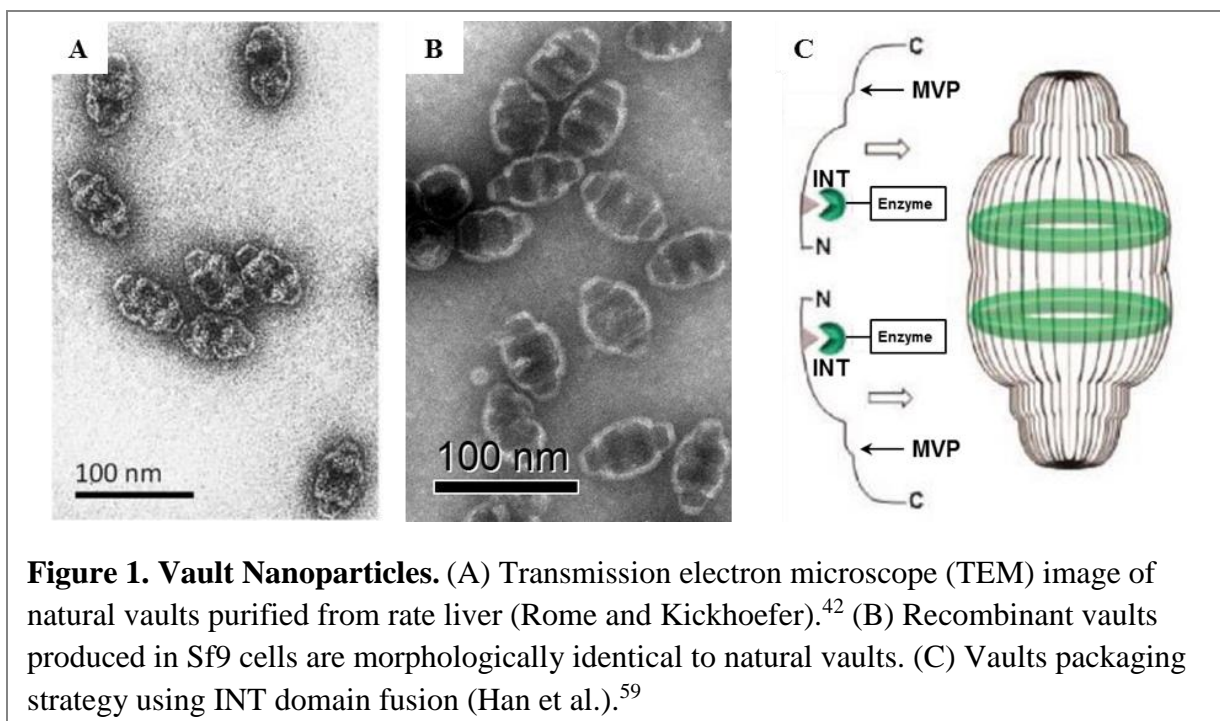
While many physico-chemical approaches are available for degradation of PFOA, such as adsorption, photooxidation, and sonochemical pyrolysis, these options tend to be energy- and cost-intensive, which are impractical and expensive to be implemented in situ for the remediation of PFOA contamination.[16-18] Bioremediation provides a cost-effective treatment alternative, and has been successfully employed in remediation of diverse contaminants, such as fluorotelomer alcohol,[19] halogenated phenols[20-22], pesticides,[23] and organic dyes.[24] Current research and practice, however, mostly focuses on treatment using microbial whole cells, which relies on microbial growth and strongly depends on water chemistries such as oxygen level, nutrient condition, co-contaminants, temperature, and pH. In addition, application of live microbial cells will also cause the concerns of potentially releasing pathogens, which pose health risk for public. The use of *in vitro* enzymes, which will eliminate the reliance of enzyme production on microbial metabolism, is a promising substitute approach, as free enzymes are more efficient, and less sensitive to the requirements for microbial growth. Recent research has shown that two enzymes including horseradish peroxidase and laccase play roles in the biodegradation of PFOA.[25, 26]

Although enzymatic bioremediation has many advantages over microbial treatment, the implementation of free enzymes for practical treatment is restricted by their stability in natural environment. *In vitro* enzymes are easily deactivated by various water chemistries, such as extreme pH, temperature, and heavy metals.[27-30] Conventional macro-sized enzyme immobilization, including surface binding and encapsulation, has been proven to be efficient for enhancing enzymatic stability. [31, 32] Through covalently binding to solid surfaces or physically entrapping in solid matrix, immobilized enzymes exhibit higher stability against various inhibitors, such as organic solvent and thermal inactivation. However, because of the strong covalent binding and extra mass transfer resistance from solid matrices, immobilized enzymes generally show lower specific activity, lower substrate affinity, and decreased turnover rates, which lead to longer remediation times..[33, 34] Recent advances in nanotechnology have provided a wide variety of nanomaterials that have the potential to promote conventional enzyme immobilization. Due to their extremely small size, the substrate diffusion resistance is minimized, which results in higher catalytic efficiency and shorter degradation times. Several types of nanoparticles have been successfully developed and employed to enhance enzymatic stability, such as nanogels,[33,

34] mesoporous silicas,[35, 36] and carbon nanotubes,[37, 38] in the past few years. Nevertheless, most of these techniques require multiple well-controlled reaction steps, which results in high cost. Additionally, these engineered nanomaterials might pose new health risk for human and wildlife.

Vault Nanoparticles

Vault nanoparticles are promising candidates to immobilize enzymes in benign vehicles and can provide a cost-effective and safe approach for *in situ* enzymatic bioremediation. Natural vaults are about 13 MDa mass, with dimensions of 41 x 41 x 72.5 nm (Figure 1A).[39-41] Since their discovery by the co-PI in 1986, vault nanoparticles have been isolated from a wide variety of eukaryotic organisms, including mice, slime molds, rabbits, cows, sea urchins, and humans, with a highly conserved morphology.[42-51] Natural vaults comprise 3 different proteins and 1 or more copies of untranslated RNAs. Inside of vault particles are multiple copies of vault poly(ADP-ribose) polymerase (VPARP also called PARP4), which contains a poly-(ADP-ribosylation) catalytic domain and a domain responsible for tightly binding to the interior of the vault shell, and several copies of telomerase-associated protein-1 (TEP1), bound to multiple copies of an untranslated vault RNA.[52-57] The Major Vault Protein (MVP), which makes up over 70% of the total vault mass, forms the outer vault shell, and is the only component needed to assemble the outer capsule of the particle. Recombinant vaults, assembled from 78 copies of heterologously expressed MVP in insect cells, have the identical morphology to natural vaults (Figure 1B).[58] Each recombinant vault particle consists of a cavity, which is large enough to hold multiple copies of macromolecules, such as protein and lipids. The INT domain, which is located at the C-terminus of VPARP, has been identified as responsible for binding to MVP. INT can be attached to heterologous proteins, and will serve as a packaging signal and subsequently direct them to the inside of the vault particle as shown in Figure 1C.[59] Moreover, MVP shell of recombinant vaults was found to be dynamic unconstrained.[60, 61] It could open partially and reversibly at the waist, or separate into two half-vaults and reassemble back rapidly, which allows the packaging of exogenous components into vaults interior *via* mixing recombinant vaults and INT fused complexes. Various components, including luciferase,[62] green fluorescent protein,[62] lipid bilayer nanodisk,[63] chemokine,[64] manganese peroxidase,[65] and membrane protein antigens [51] have been bound to the interior sites of vaults using this strategy.



Ligninolytic Enzymes

Ligninolytic enzymes are naturally produced by wood-rotting fungi, during their secondary metabolic phase of growth, as extracellular enzymes. These enzymes include, but are not limited to lignin peroxidase (LiP), manganese peroxidase (MnP), and laccase. Typically, these non-specific enzymes are secreted to break down lignin, a complex plant polymer, which is resistant to microbial degradation. Lignin is oxidized to carbon dioxide and small organic acids that can subsequently be used as carbon source for the fungi.

LiP and MnP are heme-based enzymes, while laccase is a copper-containing oxidase. Oxidation *via* LiP and MnP is initiated by the activation of peroxidase by hydrogen peroxide, resulting peroxidases to Compound I, which is a cation radical. Subsequently, compound I returns to the ground state *via* two one-electron transfer steps. H₂O is generated during the activation step and the last one-electron transfer step. For LiP, substrate could be directly oxidized by compound I and compound II, the latter of which is the reductive product of compound I after one one-electron transfer step.[66] In contrast to LiP, manganese ion (Mn²⁺) is involved to reduce MnP compound I to ground state.[67] Oxidation *via* laccase occurs at its four copper catalytic sites and is initiated by molecular oxygen oxidizing Cu(I) to Cu(II).[68] Laccase catalysis can be enhanced by adding a mediator, which donates electrons to oxidized laccase and subsequently gains electrons from the substrate.[69]

The application of peroxidases and laccase for *in situ* bioremediation is a promising technology. All three ligninolytic enzymes are non-specific enzymes and have been reported to biodegrade a wide variety of environmental contaminants, such as munitions waste,[70] chlorinated compounds,[71] polycyclic aromatic hydrocarbons,[72, 73] phenolic

compounds[74, 75] and organic dyes.[76] Recent research also found horseradish peroxidase and laccase could slowly catalyze the oxidation of PFOA.[25, 26] These degradation reactions, however, are mostly characterized in laboratory buffers rather than in real contaminated sites, because enzymes are easily affected by various field factors, such as protease, pH, temperature, and heavy metal.

Vault nanoparticles can be customized to package multiple ligninolytic enzyme proteins inside them. The vaults shell already provides a stable protective environment that may increase the stability and longevity of enzymes, without significantly limiting the diffusion of the substrates. Additionally, the compact MVP shell can prevent packaged enzymes from conformational change, and protect them from external protease digestion, and possibly enhance enzymatic stability against thermal inactivation. As compared to other nanostructure-based immobilizations requiring well-controlled conditions and serial chemical reactions steps, vault packaging can be achieved in a single step *via* mixing self-assembled empty vaults with INT fused enzymes, which makes it attractive as a green, cost-effective technology with potential for practical *in situ* bioremediation.

Materials and Methods

Enzyme Activity Assay

Enzyme activity is generally quantified in unites, and 1 unit of enzyme activity is defined as the amount of enzyme needed to react/produce 1 $\mu\text{mol}/\text{min}$ of substrate/product. Activities of fungi-produced LiP, MnP and laccase were quantified by colorimetric methods using veratryl alcohol (VA), Mn^{2+} and 2,2'-Azino-bis(3-ethylbenzothiazoline-6-sulfonic acid) diammonium salt (also called ABTS) as substrates, respectively. Hydrogen peroxide was used as the oxidant for LiP and MnP, while molecular oxygen was used in laccase catalysis. LiP catalyzes the oxidation of veratryl alcohol to veratraaldehyde, which has a strong absorbance at 308 nm (molar extinction coefficient $\epsilon = 9300 \text{ L}\cdot\text{mol}^{-1}\cdot\text{cm}^{-1}$).[77] Under the catalysis of MnP, Mn^{2+} is oxidized to Mn^{3+} , which binds with malonate ligand and generates strong absorbance peak at 270nm ($\epsilon_{270 \text{ nm}} = 11590 \text{ L}\cdot\text{mol}^{-1}\cdot\text{cm}^{-1}$).[78] ABTS, which generates green color and has strong absorbance at 420nm ($\epsilon_{420 \text{ nm}} = 36000 \text{ L}\cdot\text{mol}^{-1}\cdot\text{cm}^{-1}$)[79] when being oxidized, was used as the substrate for laccase activity measurement. For measuring activity of INT fused enzymes, ABTS was used as the sole substrate. Mn^{2+} was added as the mediator for testing the activity for recombinant MnP.

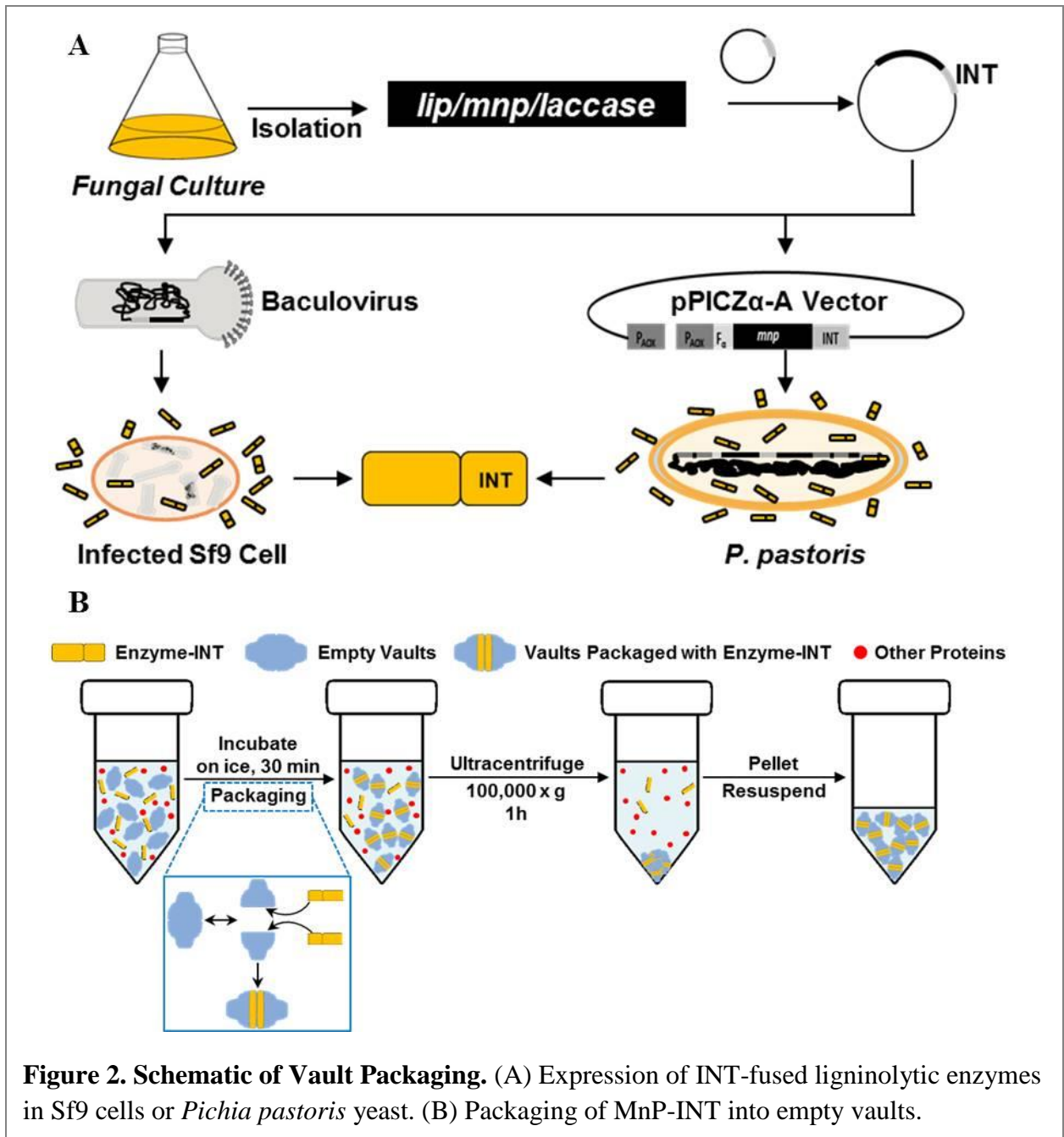
Heterologous Expression of INT Fused Ligninolytic Enzymes, and Packaging of Recombinant Enzymes into Recombinant Vaults

Phanerochaete chrysosporium (ATCC: 24725) was selected as the source of LiP and MnP enzymes, and laccase sequence was isolated from *Trametes versicolor* MAD697-R. Prior to vault encapsulation, the enzymes must undergo several molecular modifications, including addition of the INT targeting domain and removal of signal peptides as needed.

Figure 2 illustrates the scheme of vault-packaging starting from natural enzymes to vaults packaged enzymes. In brief, the coding sequences of enzymes were isolated from their source organisms, and inserted upstream of INT domain coding sequence in expression vectors. Insect Sf9 cell was selected for expression of LiP-INT and MnP-INT, while laccase-INT was expressed in *Pichia pastoris* yeast. Afterwards, the crude extract of INT-fused enzymes will be mixed with partially purified empty vaults produced in Sf9 insect cells. Due to the high affinity of INT domain to vault interior, recombinant enzymes are easily packaged into vault nanoparticles through simply mixing. Finally, ultracentrifuge was performed to separate vaults packaged with INT-fused enzymes from bulk mixture.

Cloning of Ligninolytic Enzymes Coding Sequences

P. chrysosporium is a well-known LiP and MnP producer. The fungus was cultured in nitrogen-limiting Kirk medium as previously described,[80] and collected 1 day before peroxidase activity reached its maximum observed value. *T. versicolor*, which produces laccase, was cultured in Tisma media with guaiacol as the enzyme inducer.[81] Total RNA was extracted and purified using phenol-chloroform method.[82] Subsequently, cDNA was synthesized using Thermo Scientific Maxima First Strand cDNA synthesis Kit for RT-qPCR, followed by PCR amplification using the following three sets of primers: 5'-ATGGCCTTCAAGCAGCTCT-3' and 5'-TTAAGCACCCGGAGGCG-3' for LiP, 5'-ATGGCCTTCGGTTCTCTCCTC-3' and 5'-TTAGGCAGGGCCATCGAACT-3' for MnP, and 5'-ATGTCGAGGTTTCACTCTCTTCTCGCTTT-3' and 5'-TTACTGGTCGCTCGGGTCGC-3' for laccase. PCR products were separated on agarose gel, purified and inserted into pCR4-TOPO vector (Invitrogen). Afterwards, recombinant plasmids were transferred into Mach1-T1 competent *E. coli* (Invitrogen) via heat shock, followed by ampicillin selection on LB agar. Five to ten ampicillin resistant colonies were selected, re-plated and re-grown in ampicillin containing agar or medium for each enzyme plasmid. Purified plasmids from recombinant *E. coli* culture were sequenced to confirm sequences for three ligninolytic enzymes.



Isolated LiP, MnP and laccase coding sequences are 1119 bp, 1149 bp, and 1563 bp long with 84 bp, 72 bp, and 63 bp signal sequences, respectively. INT domain fused LiP and MnP were expressed in Sf9 insect cells using pFastBac vector. For construction of intracellular expressed LiP-INT (nsLiP-INT), *lip* was amplified with a forward primer 5'-CCCCGGATCCATGGCCACCTGTTCCAACGGCAA-3', containing a *Bam*H1 restriction site, and a reverse primer, 5'-CATGCTAGCACCCGGAGGCGGAGGGA-3', containing an *Nhe*1 restriction site. PCR amplified fragments were double digested with *Bam*H1-*Nhe*1, and inserted upstream of INT-6xHis sequence in INT-6xHis-pFastBac vector treated with the

same restriction enzymes. For intracellularly expressed MnP-INT (nsMnP-INT) expression cassette, the following primers were used: forward primer with an *Bam*H1 restriction site 5'-CCCCGGATCCATGGCAGTCTGTCCAGACGGTAC-3', and reverse primer with an *Nhe*1 restriction site 5'-CATGCTAGCAGGGCCATCGAACTGAA-3'. *Bam*H1-*Nhe*1 digested PCR fragments were ligated upstream of INT-6xHis sequence in INT-6xHis-pFastbac. Extracellular expression was also performed for MnP using its own signal peptide. For construction of secreted MnP-INT expression cassette (sMnP-INT), forward primer with an *Nco*1 restriction site 5'-CTAGTCCATGGCCTTCGGTTCTCTCCTCG-3' and reverse primer with an *Nhe*1 restriction site 5'-GTGTGCAGCTAGCAGGGCCATCGAACTGAACACCAG-3' were used. PCR amplified fragments were cleaved with *Nco*1-*Nhe*1, and inserted into INT-pFastBac vector digested with the same endonucleases. Recombinant laccase-INT was expressed as secreted protein in *Pichia pastoris* yeast using pPICZ α -A vector. For construction of laccase-INT expression vector, *laccase* was amplified with a forward primer 5'-ATCGGAATTCGGTATCGGTCCCGTCGCCGA-3', containing an *Eco*R1 restriction site, and a reverse primer, 5'-TATAGCTAGCCTGGTTCGCTCGGGTTCGAGCG-3', containing an *Nhe*1 restriction site. The PCR products were digested with *Eco*R1-*Nhe*1, and inserted between alpha secretion signal sequence and INT domain coding sequence in INT-pPICZ α -A vector. All constructs were confirmed by DNA sequencing.

Expression of INT Fused Ligninolytic Enzymes

Recombinant baculovirus for expressing nsLiP-INT, nsMnP-INT and sMnP-INT were generated as described in Bac-to-Bac protocol (Invitrogen). Fifty milliliters of Sf9 cell culture (2×10^6 cells/mL, in Sf-900 II SFM media (Life Technologies)) was infected with 5 μ L baculovirus, and incubated at 27^o C. Seventy-two hours after infection, the cell pellet was collected for nsLiP-INT and nsMnP-INT analysis and the culture supernatant was collected for analysis of sMnP-INT infections. Culture supernatant containing sMnP-INT was further centrifuged at 100,000 g for 1 hour at 4 °C to remove the baculovirus particles, followed by concentrating 5-fold using an Amicon Ultracel 30KDa centrifugal filter. Subsequently, samples were analyzed by SDS-PAGE fractionation followed by both Coomassie staining and Western blot with anti-INT antibody to confirm proper expression of recombinant proteins. ABTS peroxidation assay was also performed to test peroxidase activity of INT fused LiP and MnP.

Laccase-INT was produced in *Pichia pastoris* under highly-inducible P_{AOX1} promoter, which is turned on by methanol. The expression vector was transformed into *P. pastoris* GS115 via electroporation, followed by Zeocin antibiotic selection. Afterwards, several colonies were transferred to methanol inducing plates containing ABTS to screen colonies that produced active Laccase-INT recombinant enzyme. Under the catalysis of laccase-INT, ABTS is oxidized, which generates green color and subsequently turned to dark red. Then, selected colonies were grown in glycerol medium overnight, and transferred into methanol

inducing medium for Laccase-INT production. The culture supernatant was collected every 24 hours and concentrated 5-fold using an Amicon Ultracel 30KDa centrifugal filter for testing Laccase-INT activity.

Packaging and Characterization of INT-Fused Enzymes in Vault Nanoparticles

Recombinant INT attached enzymes were packaged into vault particles through one-step mixing. Prior packaging, supernatant containing secreted INT-fused enzymes from Sf9 culture or *P. pastoris* culture were partially purified and concentrated as described above. Afterwards, processed medium containing secreted recombinant enzymes were mixed with empty human MVP vaults, and incubated on ice for 30 minutes. This was followed by centrifuging the mixture at 100,000 g for 1 hour at 4 °C. Recombinant enzymes associated with human vault nanoparticles pellets (P100), while free INT-fused enzymes would stay in the supernatant S100.

To package intracellularly expressed nsLiP-INT and nsMnP-INT into recombinant vaults, the cell lysate was mixed with CP-rMVP vaults, and purified as previously describe.[58] Resuspended pellets were analyzed by SDS-PAGE followed by Coonassie staining and Western blot using anti-INT antibodies. Transmission electron microscopy (TEM) was also performed to confirm the morphology and intactness of vault nanoparticles package with INT-fused ligninolytic enzymes. Finally, enzymatic activity of packaged vaults was assessed using ABTS peroxidation assay.

Evaluation of the Stability and Performance of Vault-Packaged Enzymes

Thermal Stability

Vault-packaged recombinant enzymes, free recombinant enzymes and fungi-produced ligninolytic enzymes were incubated at 20°C for 1 h, and then incubated at 30 °C, followed by another 1 h incubation at 40 °C. Samples were collected at 1, 2, 2.5 and 3 h, and analyzed for ABTS peroxidation activities. Residual activities were normalized to their initial activities. Additionally, to elucidate how vault packaging impacts thermal inactivation, a detailed inactivation study was performed at 25°C for 70 hours, and samples were collected at 1, 2.5, 4, 6, 8, 22, 32.5, 47, and 70.5 h. ATBS peroxidation activities were measured and normalized to their corresponding initial activities. Data obtained were fitted to the Henley inactivation model shown as following:

$$\frac{E_{obs}}{E_0} = a = \left[1 + \frac{\alpha k_1}{k_2 - k_1} \right] e^{-k_1 t} - \frac{\alpha k_1}{k_2 - k_1} e^{-k_2 t}$$

In brief, enzyme inactivation could be divided into two steps. E_0 is the initial active enzyme, and it is deactivated to E_1 , which is the less active form of the enzyme, in the first inactivation step. Subsequently, E_1 is inactivated to E_D , which is the non-active enzyme. The rate constants for two inactivation steps are k_1 and k_2 , and the ratio of specific activity of E_1 to that of E_0 is α , which is less than 1 in most cases. Values of k_1 , k_2 and α were calculated by predicting numbers that yielded the minimum sum of squared residuals.

Structural Stability of Empty Vault Nanoparticles

We next examined whether PFCs would affect the structural stability of vault nanoparticles. Empty vaults were incubated with 10 mg/L 6:2 FTUCA or PFOA in PBS buffer (pH 7.4) at room temperature. Samples were collected at Day 0, Day 1 and Day 31, and examined under TEM. Incubation of vaults in PBS buffer without PFCs was included as a control. In addition, vaults stability in PFCs contaminated groundwater that was collected from Air Force Barksdale sites, was also assessed. Table 1 summarized conditions tested for evaluating vaults structural stability.

Table 1. Experimental Conditions for Vaults Structural Stability Tests

Sample	Compound	Ethanol	Buffer
1	6:2 FTUCA	1%	PBS
2	PFOA	1%	PBS
3	-	-	PBS
4	-	-	Groundwater

Performance Under Various pH

Water chemistries vary among diver environments. The pH of surface water and groundwater ranges from 4.5 to 10, which affects the in situ enzymatic activities. To understand the performance of vault-packaged enzymes under more realistic conditions, activities of packaged enzymes, free enzymes and fungi-produced enzymes were assessed at pH ranging from 2.5 to 6.0 (0.5 gradient). Results were normalized to corresponding activity at the optimum pH.

Degradation of Perfluorooctanoic Acid

Degradation of Perfluorooctanoic Acid by Fungal Cultures

Both of *P. chrysosporium* and *T. versicolor* were exposed to PFOA. *P. chrysosporium* was pre-grown in Kirk medium[80] to accumulate biomass, and blended and resuspended in either nutrient-rich Kirk medium containing 50 g/L glucose and 5.12 g/L ammonium tartrate or nutrient-poor Kirk medium containing 20 g/L glucose and 0.2 g/L ammonium tartrate, subsequently. For *T. versicolor*, Tisma medium was used to accumulate biomass.[81] After

blending, fungal culture was resuspended in either Berg rich medium containing 8 g/L glucose and 1.584 g/L ammonium sulfate, or Hein poor medium containing 1 g/L glucose and 0.396 g/L ammonium sulfate. Ten milliliters of fungal culture were aliquoted to 125 mL serum bottles crimped with butyl stoppers. For all exposed conditions, 1 mg/L PFOA was added to each bottle. Bottles were aerated for 10 minutes when oxygen level fell below 18%. On day 0, 30, and 180, bottles were sacrificed for measuring PFOA and potential metabolites as described previously.[19] See Table 2 for a list of experimental conditions tested.

Table 2. Experimental Conditions for Fungi Exposed to PFOA

		Fungi	PFOA (mg/L)	Time Point
<i>P. chrysosporium</i>	Rich medium	Alive	1	Day 0, 30, 180
		Alive	0	Day 0, 30, 180
		Autoclaved	1	Day 0, 30, 180
	Poor medium	Alive	1	Day 0, 30, 180
		Alive	0	Day 0, 30, 180
		Autoclaved	1	Day 0, 30, 180
<i>T. versicolor</i>	Rich medium	Alive	1	Day 0, 30, 180
		Alive	0	Day 0, 30, 180
		Autoclaved	1	Day 0, 30, 180
	Poor medium	Alive	1	Day 0, 30, 180
		Alive	0	Day 0, 30, 180
		Autoclaved	1	Day 0, 30, 180

Degradation of Perfluorooctanoic Acid by In vitro Enzymes

LiP and MnP that were purified from fungus, were tested for PFOA and 6:2 FTUCA degradation at 25 °C for 200 days. Each reaction contained 1 mg/L PFOA, 1 mg/L 6:2 FTUCA, and LiP and MnP mixture. The LiP-MnP reaction mixture contained 50 mM malonate buffer (pH 4.0), LiP enzyme, MnP enzyme, 0.04 mM phenol and 1 mM MnCl₂, which were added as mediators, 1 mM veratryl alcohol, which protected LiP from being inactivated, and 0.3 mM H₂O₂. Initial LiP and MnP activities were 109.7 U/L and 414 U/L respectively. Table 3 summarized the experimental conditions tested. Samples were collected at day 0 and day 200. Prior to collection of samples, one equal volume of acetonitrile were added to terminate the reaction, and concentrations of PFOA, 6:2 FTUCA and potential metabolites were measured as previously described.[19]

Table 3. Experimental Conditions for PFOA Exposed to Fungi-Produced Enzymes

	LiP (U/L)	MnP (U/L)	VA+MnCl ₂ +H ₂ O ₂	Phenol	PFOA (mg/L)	6:2 FTUCA (mg/L)
Enzyme	109.7	414	✓	✓	1	1
	-	-	-	✓	1	1
Enzyme Free	-	-	✓	✓	1	1
	-	-	-	✓	1	1

Free and vault-packaged recombinant enzymes were also evaluated for PFOA transformation by exposing them to 10 mg/L PFOA. MnP produced by *P. chrysosporium* (nMnP) was included as a control. Reactions were performed in 50 mM malonate buffer (pH 4.5), containing MnP enzymes, PFOA, 1.5 mM MnCl₂ and 0.3 mM H₂O₂. See Table 4 a list of conditions tested. Samples were collected at day 0 and day 28 by adding 4 volumes acetonitrile to reactions, and measured for PFOA concentration using HPLC/MS/MS.[19]

Table 4. Experimental Conditions for PFOA Exposed to Three Types of MnP

	sMnP-INT (U/L)	sMnP-INT-vault (U/L)	nMnP (U/L)	PFOA (mg/L)
Enzyme	32	-	-	1
	-	32	-	1
	-	-	32	1
Enzyme Free	-	-	-	1

Results and Discussion

Cloning of Ligninolytic Enzymes Coding Genes

All coding sequences were PCR amplified and inserted into pCR4-TOPO (Invitrogen) plasmid, followed by sequencing with M13F and M13R primers. The sequencing results were blasted using the online tool blast of NCBI GeneBank to confirm the accuracy of cloned genes. Isolated LiP coding sequence was 99% identical to the CDS of ligninase

isozyme H8 gene from *P. chrysosporium* (GeneBank accession number M27401.1), and was 1119 bp long with the first 84 nucleotides belonging to the secretion signal sequence. The isolated MnP coding sequence consisted of 1149 nucleotides, which was 99% identical to the CDS of *P. chrysosporium* Mn-dependent peroxidase precursor (GeneBank accession number J04980.1). The starting codon was followed by a 72 base-pair-long leader sequence predominantly coding hydrophobic amino acids, which composed the signal peptide of MnP. Laccase coding sequence isolated from *T. versicolor* was 1563 base-pair-long, with first 63 nucleotides coding for signal sequence. GeneBank blast result showed it was 99% identical to the mRNA sequence of *T. versicolor* laccase B precursor (GeneBank accession number: XM_008034423.1). All three sequences are shown in Figure S1-3.

Heterologous Expression and Activity Test of INT-Fused Ligninolytic Enzymes

Insect Sf9 cells and *P. pastoris* were selected to produce recombinant ligninolytic enzymes. LiP-INT was expressed intracellularly in Sf9 cells, while MnP-INT was expressed as intracellular protein as well as secreted protein in Sf9 cells. INT-fused laccase was produced extracellularly using alpha signal factor in *P. pastoris*.

Expression of nsLiP-INT and nsMnP-INT

Recombinant INT-fused peroxidases were expressed in Sf9 insect cells, which were infected by baculovirus containing nsLiP-INT or nsMnP-INT coding sequences. Lysate of cell pellets, which were collected 72 hours after infection, was analyzed with Western blot using anti-INT antibody. As shown in Figure 3, INT containing proteins at a size about 55 kDa, which is consistent with the predicted sizes of nsLiP-INT and nsMnP-INT, were observed, suggesting successful intracellular expression of soluble INT-fused LiP and MnP in Sf9 cells.

Expression of sMnP-INT

Since MnP is produced as a secreted protein in fungi, the extracellular expression of INT-fused MnP was also tested in Sf9 cells. The first 72 nucleotides, coding for secretion signal sequence, were kept during cloning. Cell pellet and culture supernatant were collected from sMnP-INT baculovirus infected culture at 72 hours, and analyzed with Western blot using anti-INT antibody. While little amount of sMnP-INT was detected in cell pellet lysate, major sMnP-INT was observed in cell culture supernatant, suggesting successful expression and secretion of INT fused sMnP in Sf9 cells (Figure 4).

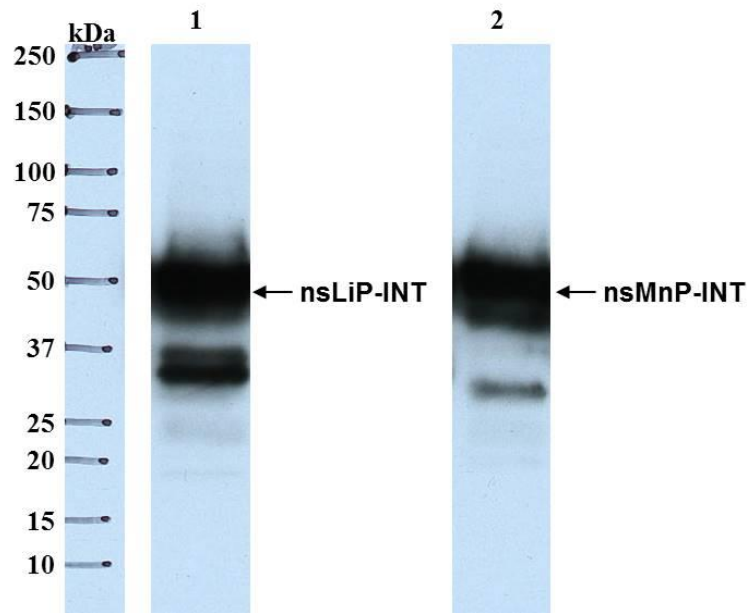


Figure 3. Western Blot Analysis of Lysate of Baculovirus Infected Sf9 Cells. Lane 1 represents nsLiP-INT lysate, and lane 2 is from nsMnP-INT lysate. The 50k bands, which are consistent with the predicted sizes of nsLiP-INT and nsMnP-INT, indicate successful intracellular expression of soluble INT-fused LiP and MnP in Sf9 cells

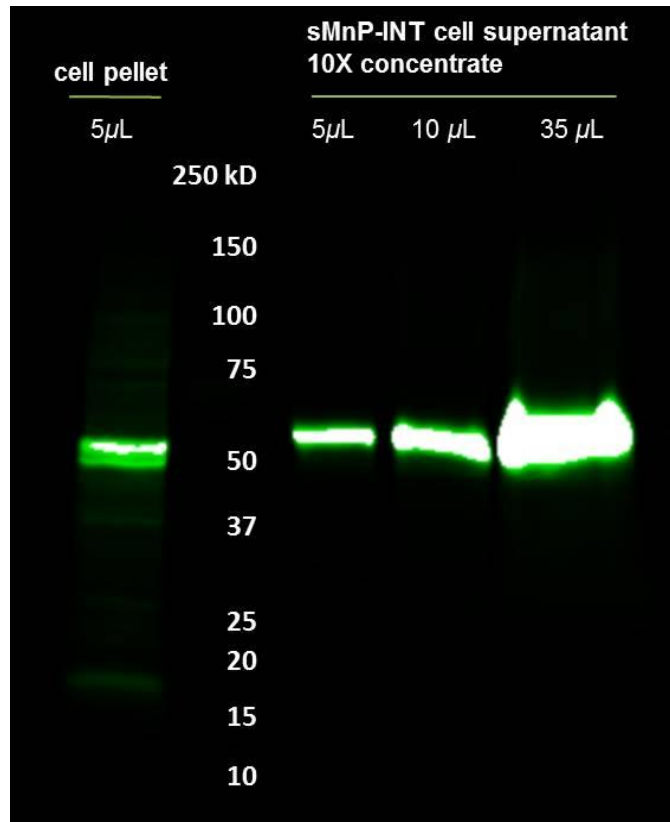


Figure 4. Western Blot Analysis of Cell Lysate and Culture Supernatant of sMnP-INT Baculovirus Infected Sf9 Cells. Major amount of sMnP-INT was detected in the culture supernatant, suggesting successful expression and secretion of INT-fused sMnP in Sf9 cells.

Expression of Laccase-INT

Yeast *P. pastoris* was chosen as the host for expressing INT-fused laccase, because expression of active several laccase isoenzymes have been achieved in this culture.[83-86] Laccase-INT expression cassette was inserted into *P. pastoris* genome *via* single crossover recombination in AOX 1 promoter. In cell, the expression of laccase-INT was regulated by the P_{AOX1}, which is turned on by methanol. To confirm the expression of active laccase-INT, a methanol plate test was performed. ABTS, which generates green or dark red color when being oxidized, was added to minimal methanol plate. Afterwards, Zeocin resistant *P. pastoris* colonies, which were transformed with laccase-INT coding sequence, were inoculated onto methanol plates and incubated at 30 °C. Due to the oxidation of ABTS under the catalysis of laccase, the colony would turn to green or dark red if it is secreting active laccase-INT. As shown in Figure 5, four of five colonies exhibited ABTS oxidation activity, while colony 5 did not generate any color change.

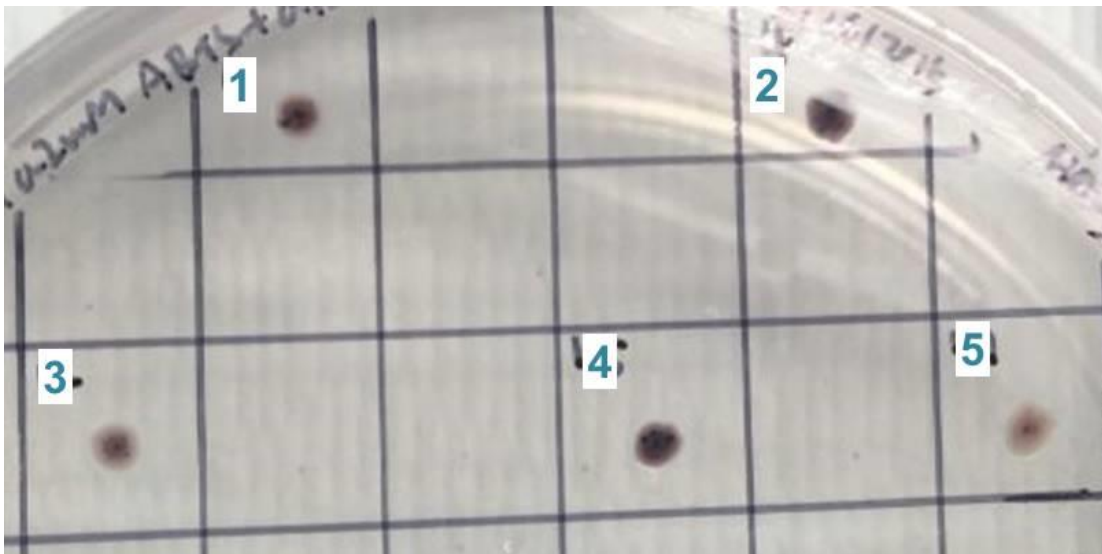


Figure 5. ABTS Oxidation Test on Methanol Plate. Colonies 1, 2, 3, and 4 generate dark red color, suggesting the production and secretion of active laccase-INT enzymes.

Activity Test of INT-Fused Ligninolytic Enzymes

Once confirmed the expression of recombinant enzymes, it was important to verify enzymes maintained their activity when fused to the INT domain and expressed heterologously. The activities of recombinant enzymes were analyzed using ABTS peroxidation assay. Under catalysis by peroxidases or laccase, the oxidation product generates a green chromophore that has strong absorbance at 420 nm, which was used for calculating enzymatic activities.

Even though transformed *P. pastoris* colonies showed ABTS oxidation activity on plates, no significant activity was observed when growing in liquid methanol medium. The INT fusion to laccase might decrease its specific activity and stability, which results in quick inactivation when being secreted into medium.

For INT-fused peroxidases expressed in Sf9 cells, oxidation of ABTS was only observed for sMnP-INT (Figure 6A), while neither nsMnP-INT nor nsLiP-INT exhibited any ABTS oxidation. Since natural LiP and MnP are produced as secreted enzymes, we reason that secretion process might contribute to correct folding of LiP and MnP and be required to activate peroxidases. Additionally, INT fused hCCL21 (human secondary lymphoid chemokine), which was secreted from infected Sf9 cells, did not shown any peroxidase activity (Figure 6B), suggesting that extracellularly expressed INT domain did not contribute to ABTS oxidation. To further confirm the ABTS oxidation activity was contributed from sMnP-INT, Mn^{2+} deplete and H_2O_2 deplete controls were performed. Fungi-produced MnP is strongly Mn^{2+} dependent and totally H_2O_2 dependent. The divalent manganese ions act as mediator between MnP and substrate, while H_2O_2 acts as the terminal electron acceptor. Ground state MnP donates two electrons to oxidant H_2O_2 , and return back *via* two steps of

one-electron transfer from Mn^{2+} . Subsequently, oxidized manganese gains electrons from substrate and drives the substrate oxidation. In the absence of Mn^{2+} , the substrate cannot directly donate electrons to oxidized MnP, resulting in little or no substrate oxidation. As shown in Figure 6A, in the absence of Mn^{2+} or H_2O_2 , no ABTS oxidation was observed for sMnP-INT. These findings indicate that extracellularly expressed sMnP-INT retained its ABTS oxidation ability even after fusion to the INT domain, and maintained its Mn^{2+} dependent property. Since secreted MnP-INT was the only active enzyme form in liquid culture, it was the only enzyme employed for further studies.

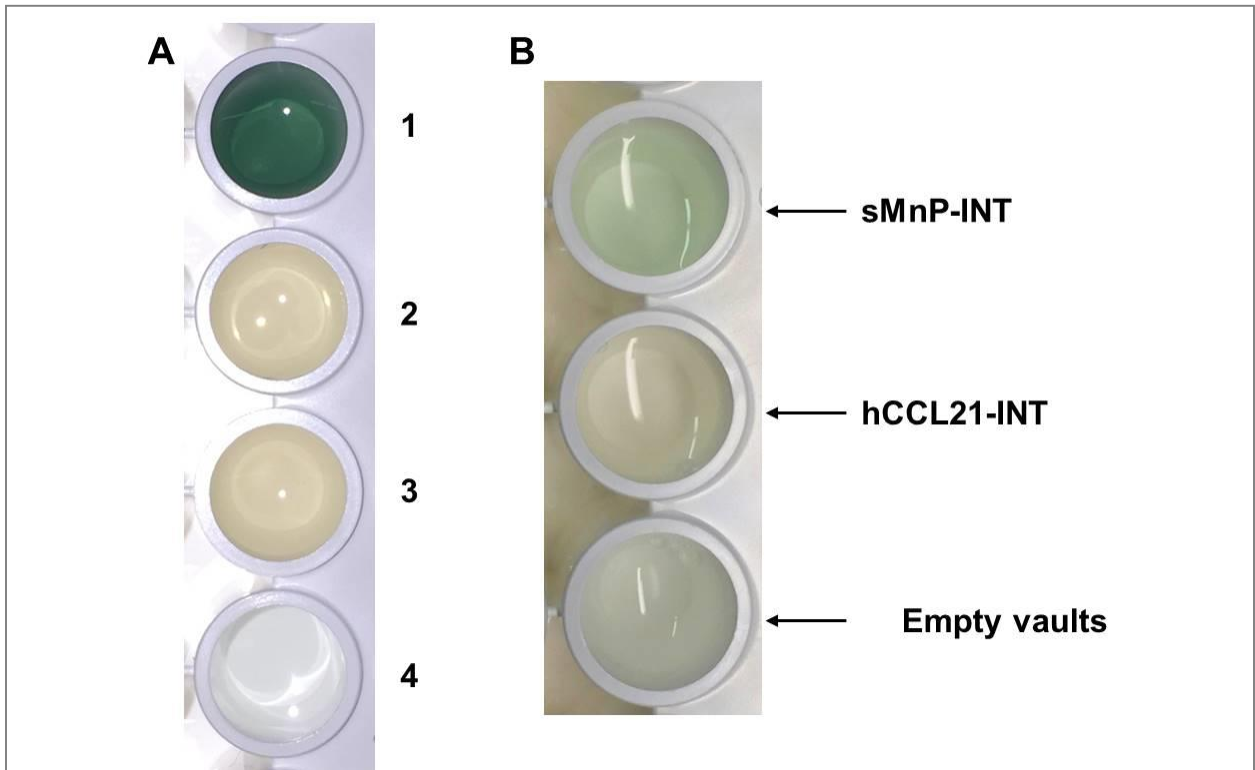
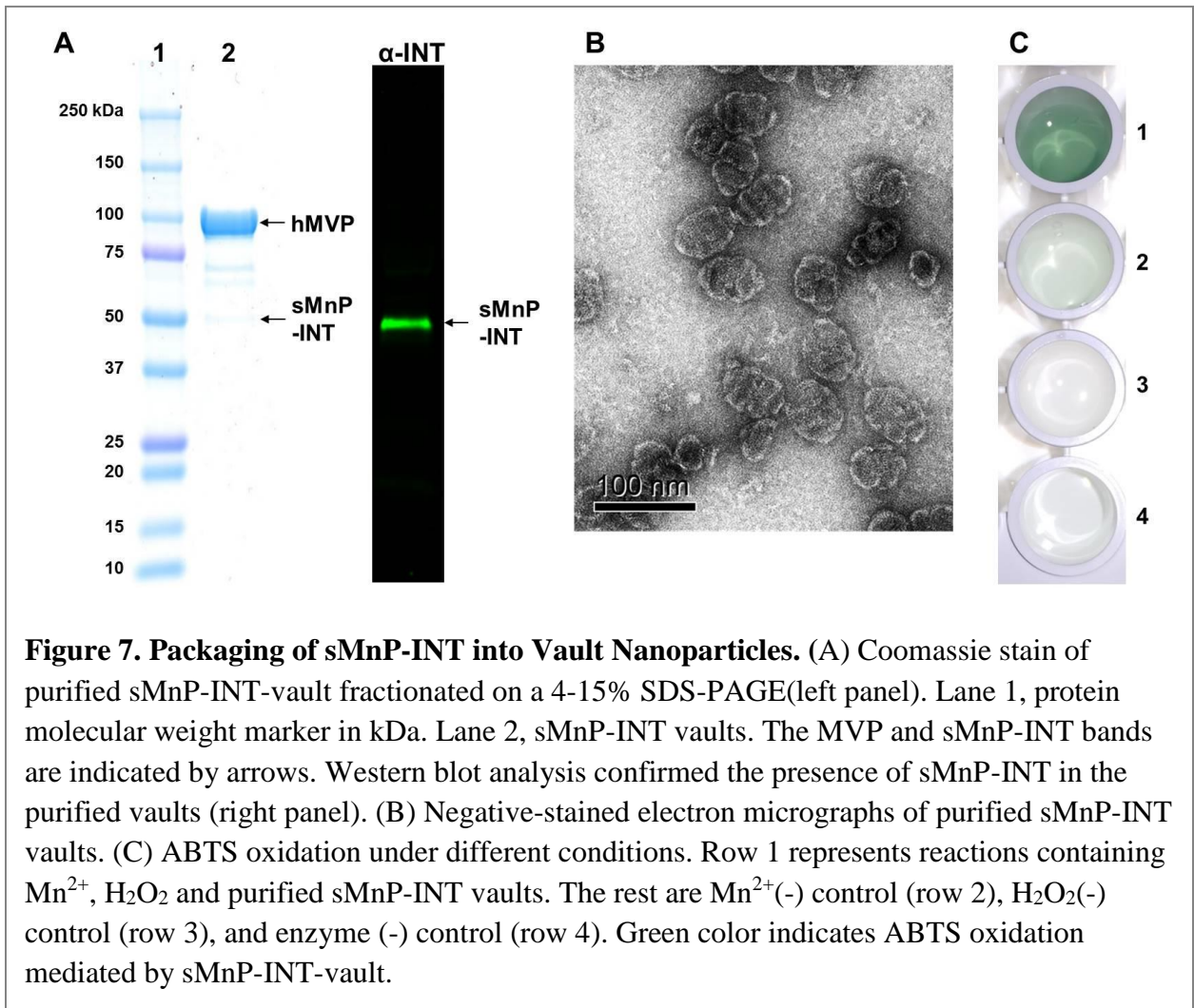


Figure 6. Peroxidase Activity Test of sMnP-INT. (A) ABTS oxidation under different conditions. Row 1 represents reactions containing Mn^{2+} , H_2O_2 and recombinant sMnP-INT. The rest are Mn^{2+} (-) control (row 2), H_2O_2 (-) control (row 3), and enzyme (-) control (row 4). Green color indicates ABTs oxidation mediated by sMnP-INT. (B) Activity tests of sMnP-INT, secreted hCCL21-INT, and empty vaults. Neither hCCL21-INT nor empty vaults showed ABTS oxidation, indicating that INT domain and vaults did not contribute to the peroxidase activity observed in sMnP-INT and sMnP-INT-vault assays.

Packaging of sMnP-INT in Vault Nanoparticles

Vaults packaged with sMnP-INT were isolated using ultracentrifuge and analyzed with Coomassie stain and immunoblot (Figure 7A). The formation of sMnP-INT vault complex indicated that sMnP-INT was successfully incorporated into vault particles. To

further confirm the formation and intactness of vault nanoparticles, purified vaults were examined with negative stain TEM. Intact vault structures, which were identical to the previously observed morphology of vault nanoparticles binding to INT fused proteins, were observed (Figure 7B), indicating that the incorporation of sMnP-INT did not affect the structural stability of vault nanoparticles. We next examined ABTS oxidation activity of vaults packaged with sMnP-INT. A significant ABTS color change was observed for vaults packaged with sMnP-INT (Figure 7C), while empty vault particles did not show any oxidation of ABTS (Figure 6B). Similar as sMnP-INT, Mn^{2+} and H_2O_2 deplete controls were also performed to further confirm the activity of vault-packaged sMnP-INT. As shown in Figure 7C, much lower oxidation of ABTS was detected for vault-packaged sMnP-INT in the absence of Mn^{2+} . Meanwhile, no oxidation was shown in H_2O_2 deplete control. These results imply that extracellularly expressed sMnP-INT could be packaged inside of vault nanoparticles without affecting the structural intactness, and could maintain its activity when packaged into vaults.



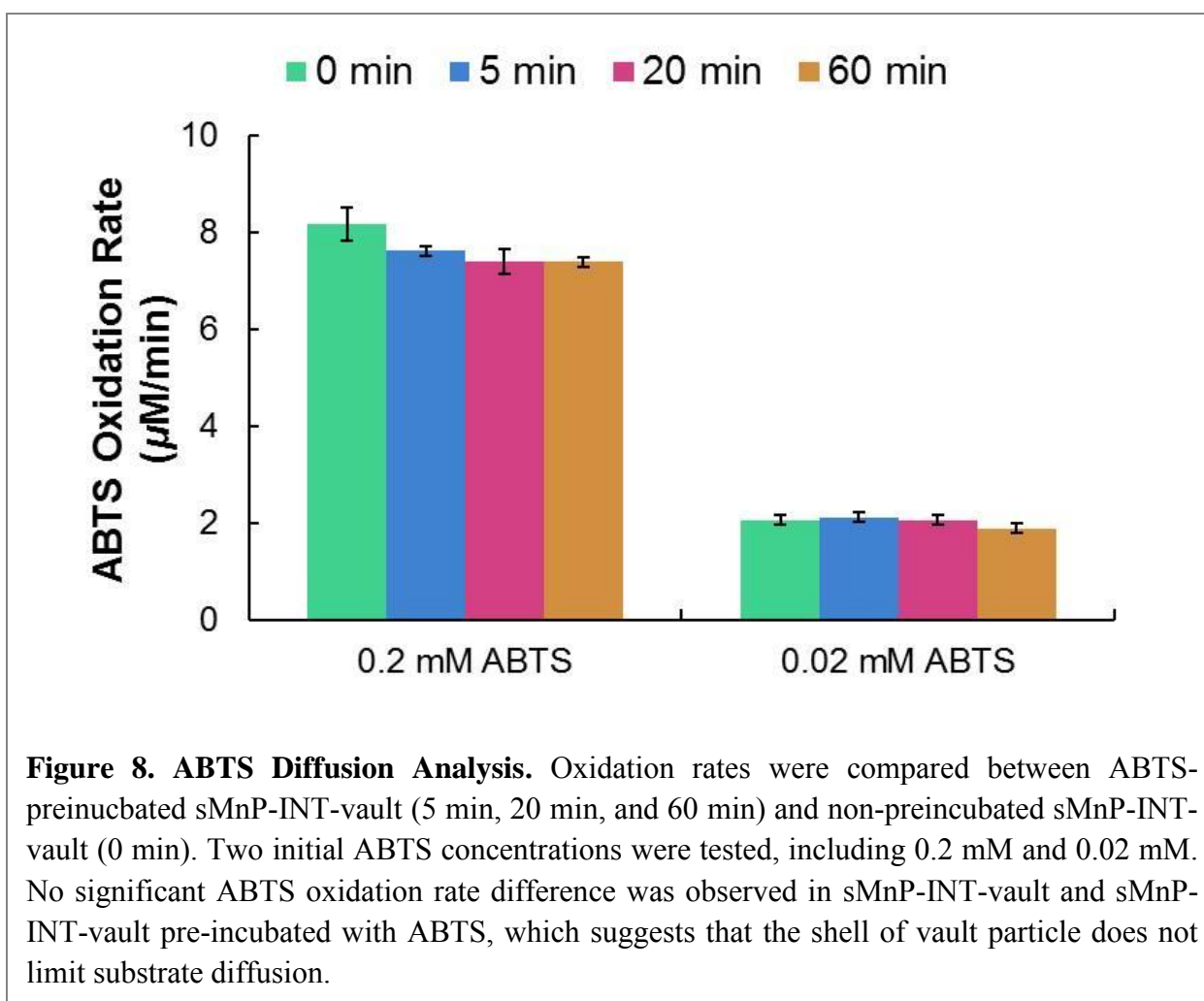
Performance of Vaults Packaged with sMnP-INT

Kinetics of sMnP-INT and Vault-Packaged sMnP-INT

The presence of the vault shell might act as a barrier that increase substrates diffusion resistance and hinder packaged enzymes from contacting with substrates, which would result in lower catalytic rate and higher apparent half-saturation constant (K_m) values. Due to the thin and dynamic MVP shell and nanoscale size of vault nanoparticles, we hypothesized that vault packaging would not significantly affect enzymatic kinetics. To validate this, K_m values of ABTS oxidation were measured for sMnP-INT and vault-packaged sMnP-INT (Table 5). MnP produced by *P. chrysosporium* was included as a control. Unexpectedly, sMnP-INT displayed lower K_m than nMnP, which means that sMnP-INT has a higher affinity for substrate ABTS. Moreover, unlike traditional enzyme packaging, resulting in marked rise of K_m values, vault-packaged sMnP-INT exhibited a K_m of 70 μM , which was only slightly higher than that of unpackaged sMnP-INT (21 μM). To further elucidate the reason for the small K_m increase in vault-packaged sMnP-INT, we examined the oxidation of ABTS preincubated with sMnP-INT-vault. A previous study found that vault-packaged luciferase showed a lag phase in luminescence intensity after initiating with ATP, while ATP preincubated luciferase-vaults displayed an immediate emission intensity rise, which suggests that the vault shell could slow down the diffusion ATP molecule and limits the availability of sequestered luciferase. Vault-packaged sMnP-INT and ABTS pre-incubated sMnP-INT-vault, however, did not show significant difference in oxidation rate (Figure 8). This result implies that, unlike ATP involved reaction, the ABTS diffusion does not limit sMnP-INT-vault catalyzed oxidation rate. Perhaps the slight increase of K_m is attributed to the binding of sMnP-INT to vaults. Overall, these findings indicate that INT domain fusion enhances the affinity of MnP to ABTS and packaging in vaults does not significantly impact substrate accessibility.

Table 5. K_m Values of sMnP-INT, sMnP-INT-vault, and naturally-produced MnP from the fungus *Phanerochaete chrysosporium*. All values were calculated from linear regression of Lineweaver-Burk Plot ($r^2 \geq 0.99$).

	K_m (μM)
sMnP-INT-vault	69.5 \pm 9.7
sMnP-INT	21.0 \pm 2.0
nMnP	102.9 \pm 9.8



Thermal Stability of Vault-Packaged sMnP-INT

The stability of packaged and unpackaged sMnP-INT against thermal inactivation was examined to test the hypothesis that vault-packaging could enhance enzymatic stability. Vault-packaged sMnP-INT, sMnP-INT, and nMnP were sequentially incubated at 20°C, 30°C and 40°C for one hour each, and residual activities were measured using ABTS oxidation and normalized to corresponding initial activities (Figure 9). As compared to unpackaged sMnP-INT and nMnP, vault-packaged sMnP-INT underwent much slower heat-induced activity losses. At 20°C, sMnP-INT lost 20% activity in 1-hour incubation, while vault-packaged sMnP-INT and nMnP still maintained 100% of their initial activity. After followed 1-hour incubation at 30°C, compared with only 45% activity retention of nMnP, vault-packaged sMnP-INT still preserved 75% of its initial activity. Subsequently, the three MnPs were incubated at 40°C. In contrast to the complete loss of activity by the nMnP and the sMnP-INT, sMnP-INT packaged in vaults still conserved 16% of its original activity. These results demonstrate that the protection of the vault shell could indeed enhance the thermal stability of packaged sMnP-INT.

To further understand how vault packaging impacts thermal inactivation, a detailed inactivation study was performed at 25°C for about 70 hours (Figure 10). Among three types of enzymes, vault-packaged sMnP-INT showed best stability, followed by nMnP, which was consistent to the sequential incubation results. The activity of unpackaged sMnP-INT decreased to half in 2.5 hours, and nearly dropped below detection limit in 50 hours. In comparison, the half-life of nMnP was about 14 hours, which is 6 times longer than that of sMnP-INT, and it still maintained 35% of its original activity after 70 hours of incubation. For vault-packaged sMnP-INT, its activity leveled off at 65% of the initial activity after 12 hours without any further significant activity loss. These collected data were fit into enzyme inactivation model previously described in Materials and Method Section. Three parameters (k_1 , k_2 and α) were calculated each type of MnP (Table 6). The sMnP-INT exhibited approximately 7 times higher k_1 and k_2 than nMnP, suggesting that INT fusion results in less stable MnP folding, and faster inactivation. This might also be the reason why the activity of laccase-INT was below detection limit in liquid medium, although it showed activity on methanol plates. It was also found that k_1 of vault-packaged sMnP-INT was slightly lower than that of sMnP-INT, and α value of sMnP-INT-vault was larger than that of sMnP-INT. Moreover, vault-packaged sMnP-INT had a 200 times smaller k_2 than free sMnP-INT. During enzyme inactivation, the first step, where initial active enzyme E_0 deactivates to less active enzyme E_1 , is mostly due to the change of sensitive structures, such as broken disulfide bonds.[87-89] The intermediate E_1 has disordered side-chain, but it still has intact backbone chain and secondary structure as E_0 . The second inactivation step, however, involves significant conformational change, which results in disordered secondary structure in non-active enzyme E_D . The slightly smaller k_1 and larger α of sMnP-INT-vault suggests that vault packaging could slow the first inactivation step and enhance activity of the intermediate E_1 . More importantly, the much lower k_2 of vault-packaged sMnP-INT indicates

vaults shell could prevent packaged enzymes from conformational change and disordering of their secondary structure. Overall, these findings illustrate that packaging in vault nanoparticles could significantly enhance enzymatic stability against thermal inactivation by providing restriction for conformational change.

Structural Stability of Vault Nanoparticles

To further evaluate the feasibility of applying vault nanoparticles in the field, we next examined the structural stability of vaults in PBS buffer (pH 7.4) containing PFCs and groundwater collected from several locations at Barksdale Air Force Base, which are contaminated with PFCs. As shown in Figure 11, no significant difference in vault morphology was observed between any of the 4 different conditions at Day 0 and Day 1, indicating that neither PFCs nor groundwater would affect vaults' structure immediately. After 31 days incubation, vault nanoparticles incubated in PBS and PBS containing PFCs showed similar morphology. Dissociation of some vault nanoparticles was observed in all three conditions, which is normal for any organic macromolecule. For vaults incubated in groundwater, no intact nanoparticle was observed probably due to interference from other organic or inorganic components, such as ions or soluble microbial products. These results confirm that PFCs do not have any impact on vaults' structural stability in 31 days, and groundwater has minimal impact the structure of vault particles.

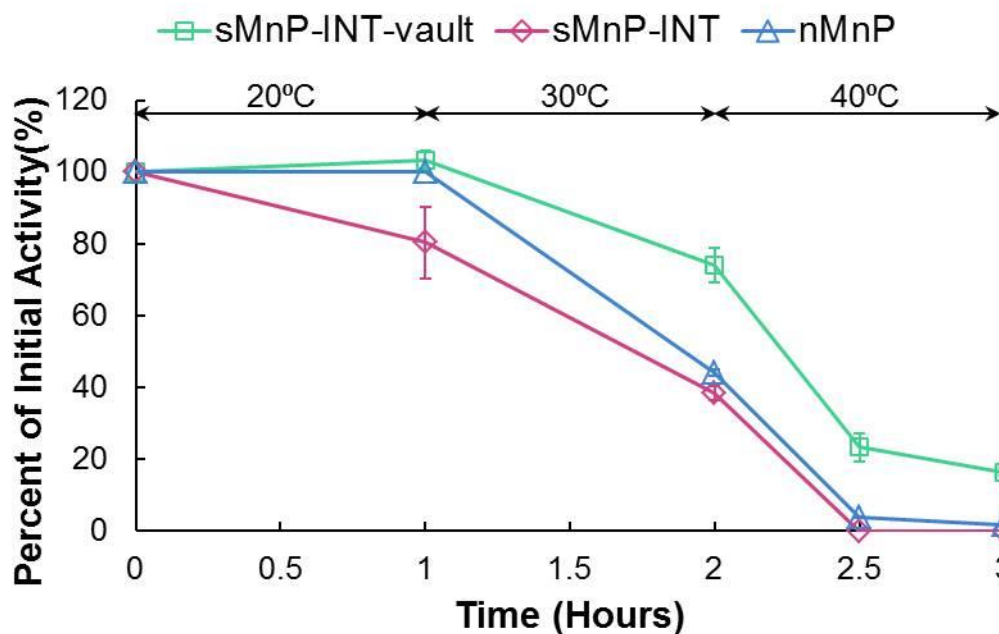


Figure 9. Enhanced Thermal Stability of Vault-packaged sMnP-INT. sMnP-INT-vault, sMnP-INT, and nMnP were incubated at 20⁰C for 1 hour, followed by 1-hour incubation at 30⁰C, and one more hour at 40⁰C. Samples were collected and analyzed over time, and activity was normalized to their initial activity.

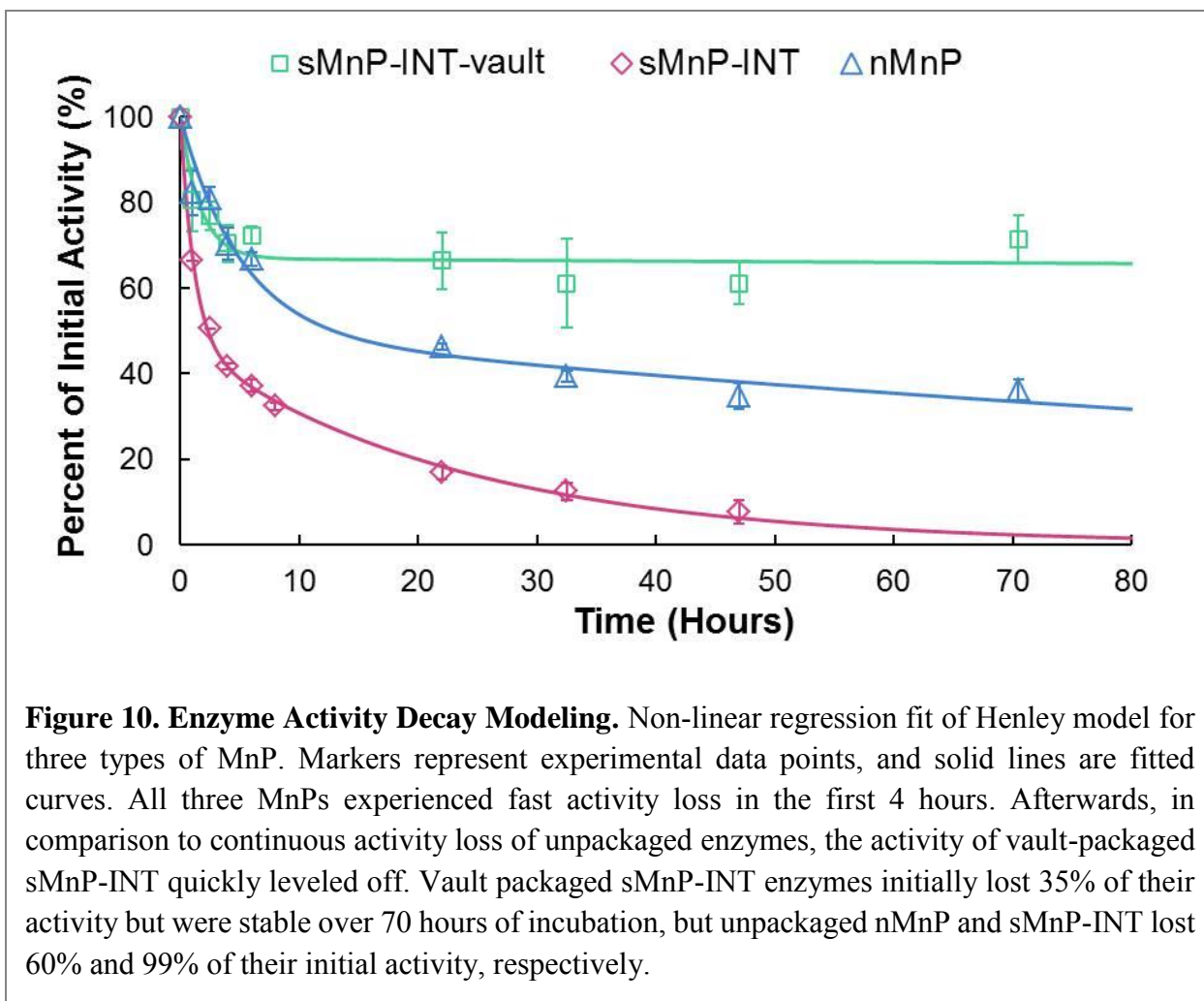
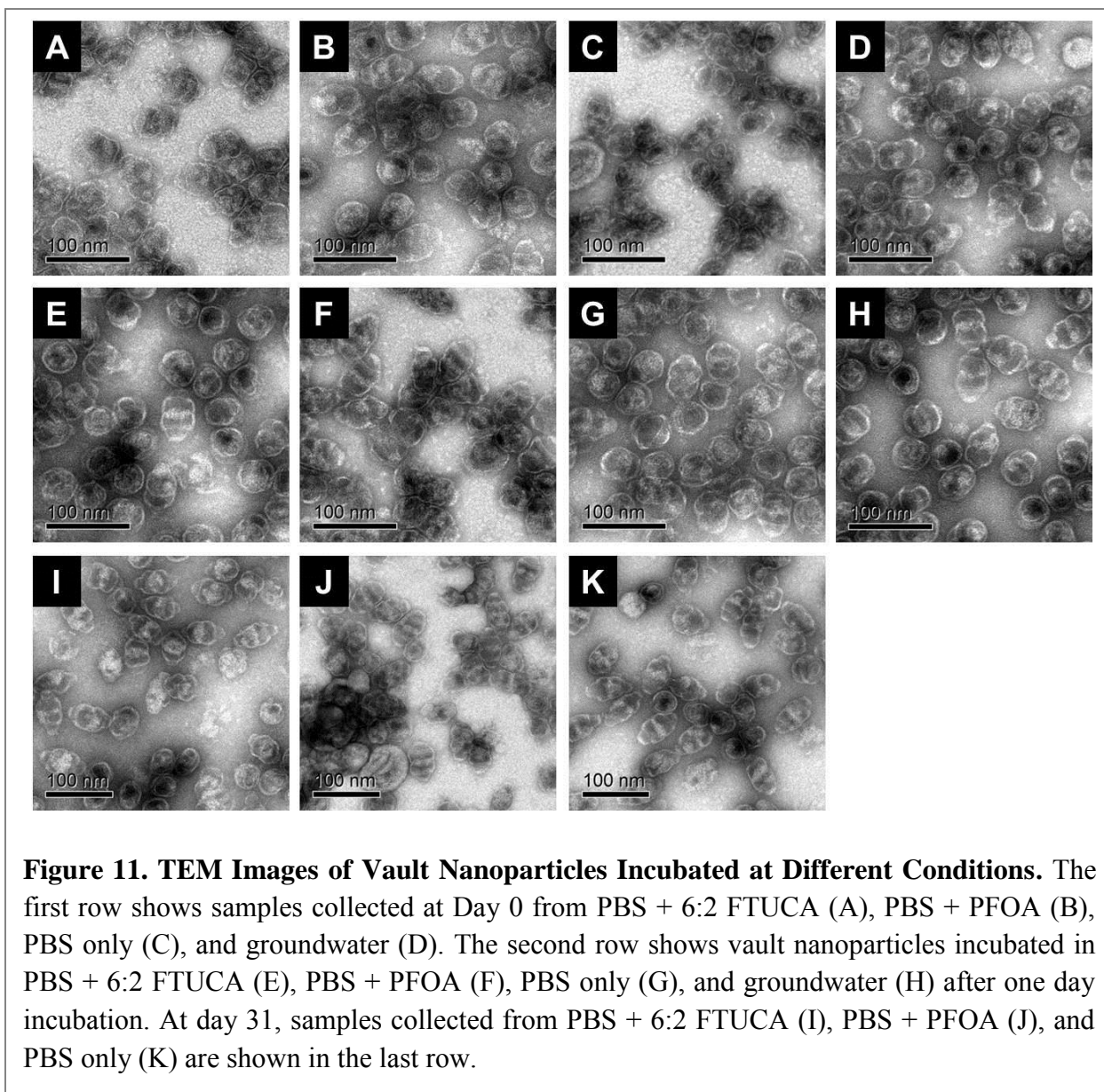


Table 6. Values of k_1 , k_2 and α for sMnP-INT, sMnP-INT-vault, and Naturally-produced MnP from the fungus *Phanerochaete chrysosporium*

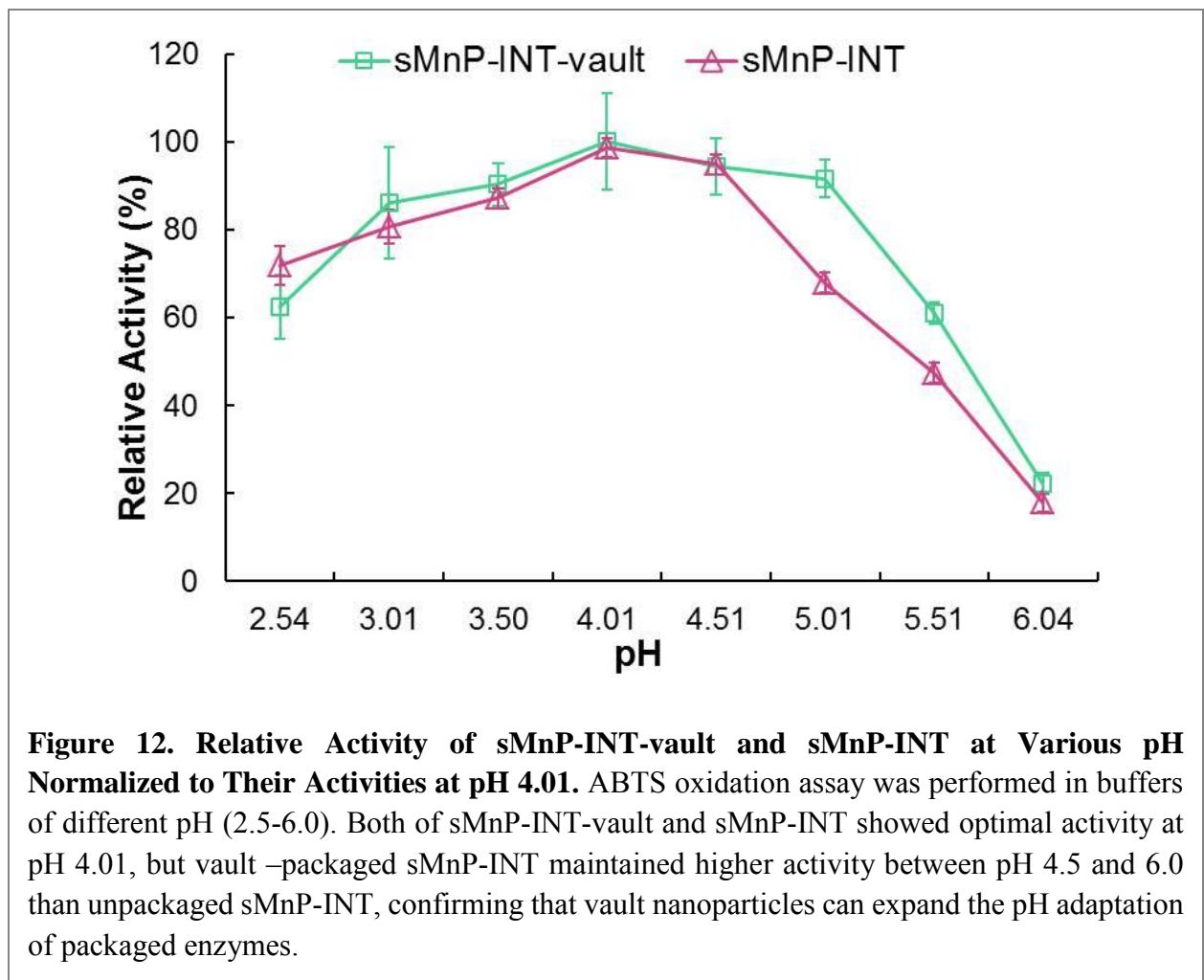
	k_1 (hr ⁻¹)	k_2 (hr ⁻¹)	α
sMnP-INT-vault	0.6	0.00021	0.67
sMnP-INT	0.86	0.043	0.45
nMnP	0.20	0.0056	0.48



Activity of Vault-Packaged sMnP-INT at Various pH Values

The pH in groundwater and surface water ranges from 4.5 to 10, which affects the in situ enzymatic activities. Previous study found the activity of MnP produced by *P. chrysosporium* was favored in weakly acidic environments (pH 4.0-5.0).[90] To understand the effects of vault-packaging on enzymatic performance under realistic conditions, we examined the activity of sMnP-INT-vault and sMnP-INT under various pH. Results were

normalized to their activity at optimal pH. As shown in Figure 12, both vault-packaged and free sMnP-INT gave the best performance at pH 4.01. At pH 5.01, sMnP-INT packaged in vaults still maintained 92% of its optimal activity, while the relative activity of unpackaged sMnP-INT decreased to 68%. When pH increased to 5.51, as compared to the 47% relative activity left in sMnP-INT, vault-packaged sMnP-INT still retained 61% of its activity at optimal pH. However, no significant activity enhancement was observed with vault-packaging when pH dropped below 3.0, which is probably due to the disassociation of vault nanoparticles in acidic solution.[91] This finding indicates that intact vault nanoparticles can enhance the activity of packaged sMnP-INT against large pH changes.



Biodegradation of Perfluorooctanoic Acid

Degradation of Perfluorooctanoic Acid by Fungal Cultures

When *P. chrysosporium* was exposed to 1 mg/L PFOA, there was no indication of PFOA transformation in 180 days. For nutrient-rich medium that supports growth for more

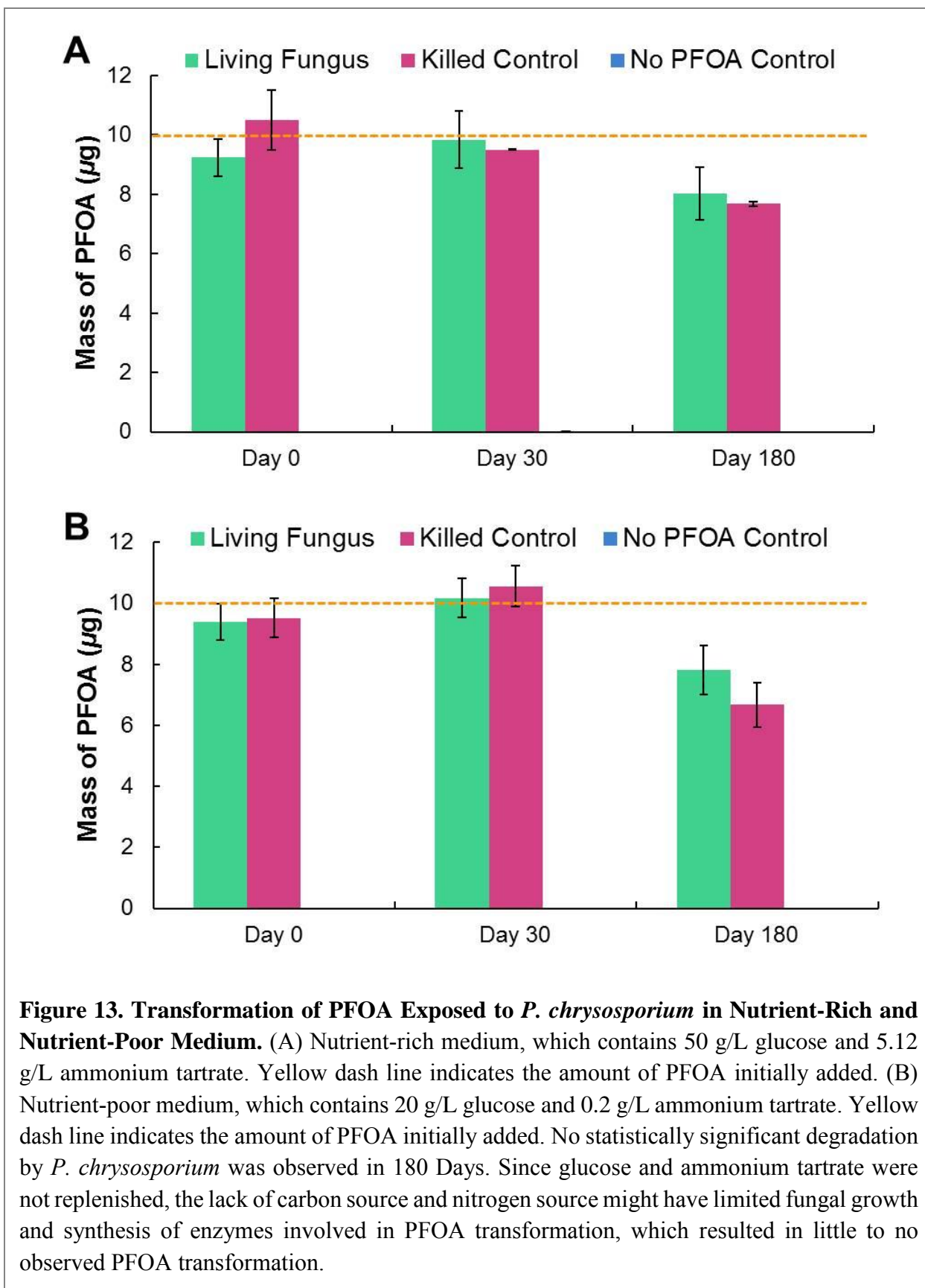
biomass, the amount of PFOA recovered from living fungus and killed control on Day 0 were $9.24 \pm 0.62 \mu\text{g}$ and $10.50 \pm 1.01 \mu\text{g}$, which were similar as the mass of PFOA added (Figure 13A). The slight decrease in PFOA amount attributes to inaccurate addition of chemicals in experiment setup. On day 30, the amount of PFOA recovered from living fungus was roughly same as it from killed control and samples on day 0, which indicates that PFOA was not transformed during 30 days incubation. After 180 days culturing, the mass of PFOA extracted from living fungus and killed control were $8.03 \pm 0.90 \mu\text{g}$ and $7.68 \pm 0.07 \mu\text{g}$, respectively, which were 10-20% lower than the amount of initially added PFOA. The loss of recovered PFOA may be due to the evaporation in aeration and incubation. As compared to PFOA mass in the killed control, similar amount of PFOA was recovered from living fungus, which suggests *P. chrysosporium* cannot transform PFOA in rich medium. PFOA was not detected on day 0, 30 or 180 in no PFOA control, indicating that it was not formed in living culture. Nutrient-poor medium, which induces production of LiP and MnP,[80] was also included for testing whether peroxidase can work on PFOA. As shown in Figure 13B, similar results were observed. No significant difference was observed between live fungus samples and killed controls. On day 0 and day 30, recoveries of PFOA were around 100%. However, only 65-75% PFOA was recovered on day 180, which may be due to the evaporation during aeration and incubation. Amount of PFOA in no PFOA controls was below detection limit, indicating *P. chrysosporium* cannot produce PFOA in poor medium either.

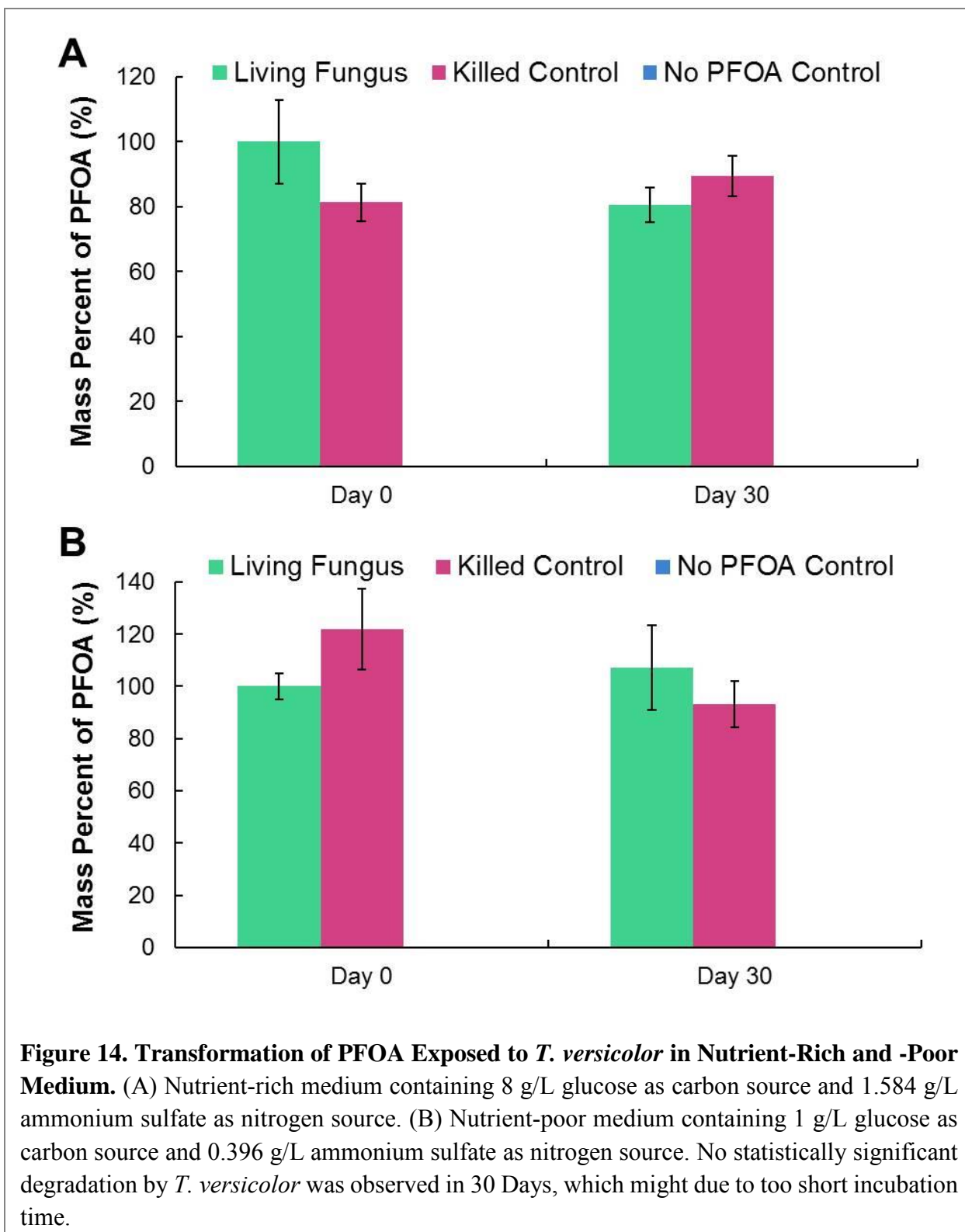
For *T. versicolor*, there was no significant degradation of PFOA in 30 days either (Figure 14). Berg nutrient-rich medium, which strongly introduced laccase production (Figure S4), did not support PFOA transformation, indicating that laccase could not catalyze the oxidation of PFOA under the experimental conditions.

Degradation of Perfluorooctanoic Acid by In vitro Enzymes

The negligible transformation of PFOA in *P. chrysosporium* culture might have been due to non-optimal conditions for peroxidase catalysis and lack of the oxidant, H_2O_2 . Thus, we next examined the transformation of PFOA catalyzed by vault-packaged sMnP-INT, free sMnP-INT as well as nMnP. The initial concentration of PFOA was approximately 10 mg/L. After 28 days incubation, the concentration of PFOA was not statistically different from initial concentration (Figure 15), which indicates none of three types of MnP individually could catalyze the initial steps of PFOA transformation under the test conditions.

Previous studies, which observed PFOA degradation under the catalysis of ligninolytic enzymes,[25, 26] either used much higher enzymatic activity or incubated the reactions for much longer period with replenishing enzymes. This experiment was performed at low enzymatic activity without any replenishment of enzymes and much shorter time period, which might be the reason why little to no PFOA transformation was observed.





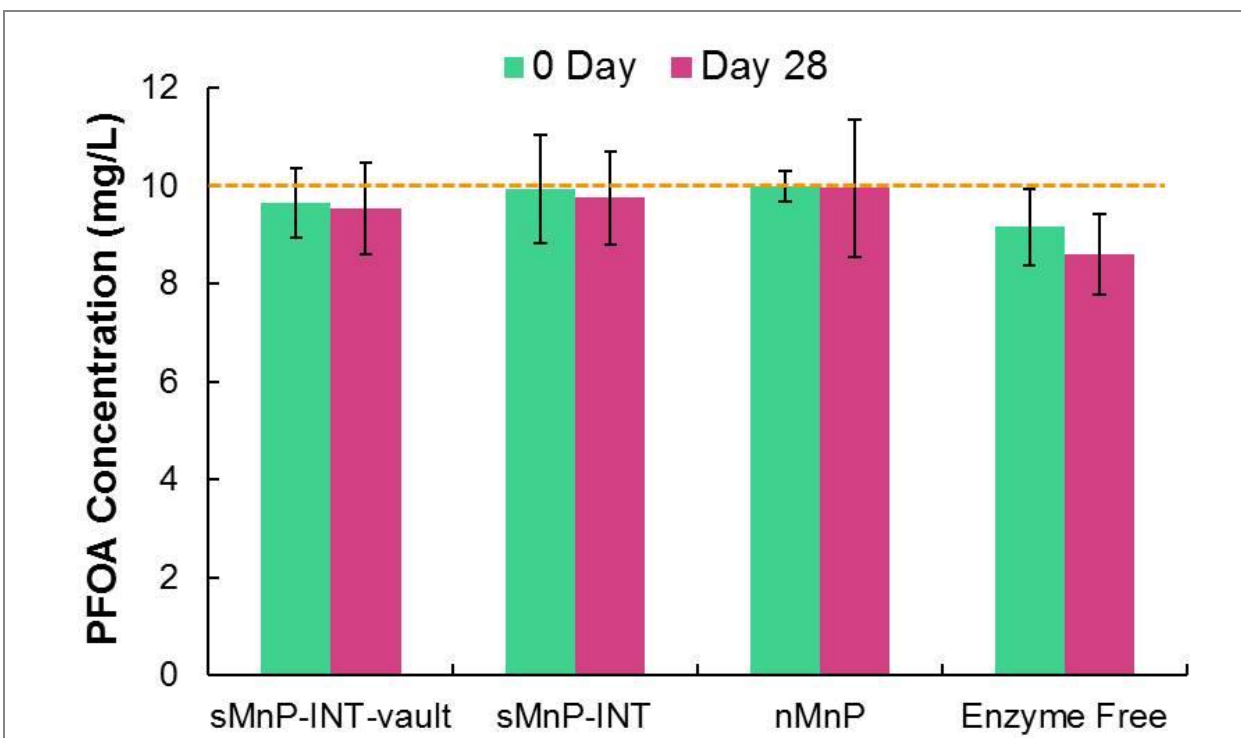


Figure 15. Transformation of PFOA Exposed to Vault-Packaged sMnP-INT, Unpackaged sMnP-INT and nMnP. Enzyme free condition was included as negative controls. The yellow dash line indicates initial PFOA concentration. No significant PFOA degradation was observed after enzyme treatment. The possible causes might be too short incubation times, very low amounts of enzymes used in the reactions, incorrect selection of MnP enzyme, and other experimental errors, including abiotic losses, and analytical limitations.

Conclusions and Future Research Directions

This project serves as the foundation for developing an innovative bioremediation technology using vault nanoparticles packaged with enzymes. This was a new application of a tool already successfully used in the medical field. This technology will ultimately reduce time and costs of environmental restoration by increasing the longevity of the biodegradative enzymes and eliminating the need for advanced chemical transformation processes or bioaugmentation with live microbes. Furthermore, packaging contaminant-degrading enzymes into vaults can lead to dynamic molecular-engineered solutions for *in-situ* remediation. These solutions include vault modifications to increase their affinity to target compounds and to improve their effectiveness in complex contaminated environments. In addition, if one or more enzymes involved in biodegradation of multiple co-contaminants are packaged inside vaults, such vaults can potentially be a “one stop shop” for removing a suite of groundwater contaminants, increasing the incredible versatility of vaults beyond the scope of our proposed research.

In this 1-year long limited scope project, INT domain fused ligninolytic enzymes were heterologously expressed in Sf9 insect cells or *P. pastoris* yeasts. Extracellularly expressed MnP-INT was determined to be the only recombinant enzyme that had detectable activity in liquid medium. The sMnP-INT was successfully packaged into empty vaults *via* simple mixing, and retained its peroxidase activity when being packaged. Recombinant vaults packaged with sMnP-INT showed identical morphology as empty ones, suggesting packaging of INT fused MnP does not affect their structural intactness. In contrast to the significant K_m increases observed in macro-sized immobilization methods, vault-packaged sMnP-INT showed just marginally higher K_m than free sMnP-INT. Further thermal stability study revealed that vault-packaging could significantly enhance sMnP-INT stability *via* constraining enzymes from conformational changes. The structural intactness of empty vaults was confirmed by incubation in the presence of PFCs in 1 month in PBS buffer. Additionally, it was found that intact vault nanoparticles improved the activity of packaged sMnP-INT against large pH changes.

Using fungal cultures as well as vault-packaged sMnP-INT, free sMnP-INT and nMnP, little to no PFOA transformation was measured. Previous studies that reported PFOA degradation by horseradish peroxidase and laccase were performed at nearly three orders of magnitude higher activity and over 180 days, with very frequent replenishment of the enzymes and addition of mediators. Due to the limitations of vault production during the project duration, PFOA transformation by *in vitro* enzymes in this project was only conducted for 28 days at low enzymatic activity. To confirm PFOA degradation, higher activity and/or longer time should be tested. In addition, the absence of mediators could be another reason why significant PFOA degradation was not observed.

The results of this project encourage future fundamental research on designing multi-enzyme packaged vault particles as well as direct application of packaged vaults for *in situ*

remediation of environmental contaminants. We propose to continue this research direction with expanded scope to include (1) evaluating biodegradation of other contaminants previously reported to be catalyzed by MnP, (2) packaging of multiple enzymes within a vault, (3) increasing the scale of manufacturing, immobilization, and distribution of vault particles, and (4) comprehensive characterization of vault performance in environmental microcosms to move towards field demonstration.

MnP has been previously reported to catalyze a broad range of target contaminants, such as RDX[92] and multiple phenolic compounds,[93] which are detected in soils, surface water, and groundwater at many sites. Using these systems already prepared and validated in our study, we propose to extend the application of the vault nanoparticles packaged with active MnP to degrade RDX, polybrominated diphenyl ethers (PBDEs), and other emerging contaminants, such as bisphenol A, bisphenol S, nonylphenol, triclosan, etc.

The potential to encapsulate multiple enzymes within a single vault particle is a promising feature of packaged vaults. Development of this approach would allow the simultaneous transformation of contaminant mixtures such as petroleum hydrocarbons, chlorinated solvents, or other compounds commonly detected at DoD sites. We propose to build upon the procedures developed in the limited scope study to package other specific biodegradative enzymes, such as methane monooxygenase, dioxane monooxygenase, reductive dehalogenases, or perchlorate reductase, into vault nanoparticles for more customized enzyme catalyzed solutions for treating contaminated sites.

Further studies will center on large scale manufacturing of packaged vaults to meet the requirements of field demonstration. Current production of vault particles, accomplished in baculovirus infected insect cells, is costly, and has limited potential for industrial manufacturing. The yeast *Pichia pastoris* expression system, which is being used successfully for the production of various recombinant proteins, is a promising cost-effective alternative to baculovirus expression system, which will allow simple integration of vault-enzymes into industrial manufacturing systems and would allow vault enzyme prototypes to be rapidly and cost-effectively scaled up and deployed for specific environmental remediation targets.

For more effective *in-situ* performance, we propose to use vaults that are naturally abundant in a common soil organism, *Dictyostelium discoideum*, which can be cultured in large quantities for the large-scale production of vaults. *D. discoideum* is a non-pathogenic slime mold indigenous to diverse soils. It naturally generates over ten thousand vault particles per cell[46, 94] that can be easily harvested.[95] The research team will explore the feasibility of using *D. discoideum* to simultaneously manufacture and package vaults with biodegradative enzymes *in vivo*. The distribution of packaged vaults may be aided by the abundance of *D. discoideum* organisms and their dispersing spores. The natural spreading of packaged vaults can potentially allow remediation of a large contaminated site. Additionally, *D. discoideum* can enhance production of packaged vaults while further protecting enzymes from environmental conditions.

Overall, this project will serve as the foundation for integration of vaults with specific biodegradative enzymes in a transformative step towards effective *in situ* bioremediation of

environmental contaminants with the potential for more customized enzyme catalyzed solutions for treatment of contaminated sites.

Publications and Presentations

1. Wang, M.; Abad, D.; Kickhoefer, V. A.; Rome, L. H.; Mahendra, S. (2015). Vault Nanoparticles Packaged with Enzymes as an Efficient Pollutant Biodegradation Technology. *ACS Nano* 9: 10931-10940.
2. Wang, M. (2015). Peroxidase Enzymes Packaged in Vaults as an Innovative Bioremediation Technology. MS Thesis, University of California, Los Angeles, CA.
3. Wang, M.; Abad, D.; Kickhoefer, V. A.; Rome, L. H.; Mahendra, S. (2016). Vault Nanoparticles Packaged with Enzymes as an Innovative Pollutant Biodegradation Technology. *Emerging Contaminants Summit*, Westminster, CO.
4. Mahendra, S. (2016). Keynote: Nanoparticles in Water: Emerging Contaminants or Treatment Agents. *Emerging Contaminants Summit*, Westminster, CO.
5. Wang, M.; Abad, D.; Kickhoefer, V. A.; Rome, L. H.; Mahendra, S. (2016). Efficient Biodegradation of Bisphenol A by Enzymes Packaged in Vault Nanoparticles. *251st American Chemical Society National Meeting & Exposition*, San Diego, CA.
6. Rome, L. H.; Mahendra, S. (2016). Biological and Environmental Applications of Vaults. *Genencor/DuPont Industrial Biosciences*, Palo Alto, CA.
7. Wang, M., D. Abad, V. A. Kickhoefer, L. H. Rome, and S. Mahendra (2016). Enhanced Biodegradation of Bisphenol A Using Vault Nanoparticles Packaged with Enzymes. *Tenth International Conference on Remediation of Chlorinated and Recalcitrant Compounds*, Palm Springs, CA.
8. Wang, M.; Abad, D.; Kickhoefer, V. A.; Dunn, B.; Rome, L. H.; Mahendra, S. (2016). Sol-gel Immobilized Vault Nanoparticles for Water Treatment Applications. *American Chemical Society 252nd National Meeting & Exposition*. Philadelphia, PA.
9. Mahendra, S. (2016). Vault Nanoparticles Packaged with Enzymes as a Novel Biological Water Treatment Technology. *Department of Earth & Environmental Science Seminar, University of Pennsylvania*, Philadelphia, PA.
10. Mahendra, S. (2016). Vault Nanoparticles: A Platform Technology for Industrial and Environmental Applications. *Chemours/DuPont Technology Forum*, Wilmington, DE.

Awards

- Meng Wang, MWH/AEESP Outstanding Master's Thesis Award. Association of Environmental Engineering and Science Professors, New Orleans, LA (2016).
- Meng Wang, Certificate of Merit, American Chemical Society 251st National Meeting & Exposition, San Diego, CA (2016).
- Meng Wang, Honorable Mention in Student Paper Competition, Emerging Contaminants Summit, Westminster, CO (2016).

References

1. Smart, B. E., Characteristics of C-F Systems. In *Organofluorine Chemistry*, Banks, R. E.; Smart, B. E.; Tatlow, J. C., Eds. Springer US: 1994; pp 57-88.
2. Buck, R. C.; Franklin, J.; Berger, U.; Conder, J. M.; Cousins, I. T.; de Voogt, P.; Jensen, A. A.; Kannan, K.; Mabury, S. A.; van Leeuwen, S. P. J., Perfluoroalkyl and polyfluoroalkyl substances in the environment: Terminology, classification, and origins. *Integrated Environmental Assessment and Management* **2011**, *7*, (4), 513-541.
3. Herzke, D.; Olsson, E.; Posner, S., Perfluoroalkyl and polyfluoroalkyl substances (PFASs) in consumer products in Norway – A pilot study. *Chemosphere* **2012**, *88*, (8), 980-987.
4. Paul, A. G.; Jones, K. C., A First Global Production, Emission, And Environmental Inventory For Perfluorooctane Sulfonate. *Environ Sci Technol* **2009**, *43*, (2), 386-392.
5. Place, B. J.; Field, J. A., Identification of Novel Fluorochemicals in Aqueous Film-Forming Foams Used by the US Military. *Environ. Sci. Technol.* **2012**, *46*, (13), 7120-7127.
6. Schultz, M. M.; Barofsky, D. F.; Field, J. A., Quantitative determination of fluorotelomer sulfonates in groundwater by LC MS/MS. *Environ Sci Technol* **2004**, *38*, (6), 1828-1835.
7. Fromme, H.; Midasch, O.; Twardella, D.; Angerer, J.; Boehmer, S.; Liebl, B., Occurrence of perfluorinated substances in an adult German population in southern Bavaria. *Int Arch Occup Environ Health* **2007**, *80*, (4), 313-319.
8. Giesy, J. P.; Kannan, K., Global Distribution of Perfluorooctane Sulfonate in Wildlife. *Environ Sci Technol* **2001**, *35*, (7), 1339-1342.
9. Armitage, J. M.; MacLeod, M.; Cousins, I. T., Modeling the Global Fate and Transport of Perfluorooctanoic Acid (PFOA) and Perfluorooctanoate (PFO) Emitted from Direct Sources Using a Multispecies Mass Balance Model. *Environ Sci Technol* **2009**, *43*, (4), 1134-1140.
10. Prevedouros, K.; Cousins, I. T.; Buck, R. C.; Korzeniowski, S. H., Sources, Fate and Transport of Perfluorocarboxylates. *Environ Sci Technol* **2006**, *40*, (1), 32-44.
11. Hagenaaers, A.; Vergauwen, L.; De Coen, W.; Knapen, D., Structure–activity relationship assessment of four perfluorinated chemicals using a prolonged zebrafish early life stage test. *Chemosphere* **2011**, *82*, 764-772.
12. Hansen, K. J.; Clemen, L. A.; Ellefson, M. E.; Johnson, H. O., Compound-specific, quantitative characterization of organic: Fluorochemicals in biological matrices. *Environ Sci Technol* **2001**, *35*, (4), 766-770.
13. Kannan, K.; Corsolini, S.; Falandysz, J.; Fillmann, G.; Kumar, K. S.; Loganathan, B. G.; Mohd, M. A.; Olivero, J.; Van Wouwe, N.; Yang, J. H.; Aldous, K. M., Perfluorooctanesulfonate and related fluorochemicals in human blood from several countries. *Environ Sci Technol* **2004**, *38*, (17), 4489-4495.
14. Olsen, G. W.; Burris, J. M.; Burlew, M. M.; Mandel, J. H., Epidemiologic assessment of worker serum perfluorooctanesulfonate (PFOS) and perfluorooctanoate (PFOA) concentrations and medical surveillance examinations. *J Occup Environ Med* **2003**, *45*, (3), 260-270.

15. Jin, Y. H.; Liu, W.; Sato, I.; Nakayama, S. F.; Sasaki, K.; Saito, N.; Tsuda, S., PFOS and PFOA in environmental and tap water in China. *Chemosphere* **2009**, *77*, (5), 605-611.
16. Ochoa-Herrera, V.; Sierra-Alvarez, R., Removal of perfluorinated surfactants by sorption onto granular activated carbon, zeolite and sludge. *Chemosphere* **2008**, *72*, (10), 1588-1593.
17. Senevirathna, S. T. M. L. D.; Tanaka, S.; Fujii, S.; Kunacheva, C.; Harada, H.; Ariyadasa, B. H. A. K. T.; Shivakoti, B. R., Adsorption of perfluorooctane sulfonate (n-PFOS) onto non ion-exchange polymers and granular activated carbon: Batch and column test. *Desalination* **2010**, *260*, (1-3), 29-33.
18. Vecitis, C. D.; Park, H.; Cheng, J.; Mader, B. T.; Hoffmann, M. R., Treatment technologies for aqueous perfluorooctanesulfonate (PFOS) and perfluorooctanoate (PFOA). *Frontiers of Environmental Science & Engineering in China* **2009**, *3*, (2), 129-151.
19. Tseng, N.; Wang, N.; Szostek, B.; Mahendra, S., Biotransformation of 6:2 Fluorotelomer Alcohol (6:2 FTOH) by a Wood-Rotting Fungus. *Environ Sci Technol* **2014**, *48*, (7), 4012-4020.
20. Hofrichter, M.; Bublitz, F.; Fritsche, W., Unspecific Degradation of Halogenated Phenols by the Soil Fungus *Penicillium frequentans* Bi 7/2. *J Basic Microb* **1994**, *34*, (3), 163-172.
21. Haggblom, M. M.; Young, L. Y., Anaerobic Degradation of Halogenated Phenols by Sulfate-Reducing Consortia. *Applied and environmental microbiology* **1995**, *61*, (4), 1546-1550.
22. Buitron, G.; Gonzalez, A.; Lopez-Marin, L. M., Biodegradation of Phenolic Compounds by an Acclimated Activated Sludge and Isolated Bacteria. *Water Sci Technol* **1998**, *37*, (4-5), 371-378.
23. Gavrilescu, M., Fate of Pesticides in the Environment and Its Bioremediation. *Eng Life Sci* **2005**, *5*, (6), 497-526.
24. Renganathan, V.; Spadaro, J. T.; Gold, M. H., Degradation of Azo Dyes by the Lignin-Degrading Fungus *Phanerochaete chrysosporium*. *J Cell Biochem* **1993**, 194-194.
25. Luo, Q.; Lu, J. H.; Zhang, H.; Wang, Z. Y.; Feng, M. B.; Chiang, S. Y. D.; Woodward, D.; Huang, Q. G., Laccase-Catalyzed Degradation of Perfluorooctanoic Acid. *Environ Sci Tech Let* **2015**, *2*, (7), 198-203.
26. Colosi, L. M.; Pinto, R. A.; Huang, Q. G.; Weber, W. J., Peroxidase-Mediated Degradation of Perfluorooctanoic Acid. *Environmental Toxicology and Chemistry* **2009**, *28*, (2), 264-271.
27. Tuisel, H.; Sinclair, R.; Bumpus, J. A.; Ashbaugh, W.; Brock, B. J.; Aust, S. D., Lignin Peroxidase H2 from *Phanerochaete chrysosporium*: Purification, Characterization and Stability to Temperature and pH. *Archives of Biochemistry and Biophysics* **1990**, *279*, (1), 158-166.
28. Mao, L.; Huang, Q.; Lu, J.; Gao, S., Ligninase-Mediated Removal of Natural and Synthetic Estrogens from Water: I. Reaction Behaviors. *Environ Sci Technol* **2009**, *43*, 374-379.
29. Park, J. W.; Dec, J.; Kim, J. E.; Bollag, J. M., Effect of Humic Constituents on the Transformation of Chlorinated Phenols and Anilines in the Presence of

- Oxidoreductive Enzymes or Birnessite. *Environ Sci Technol* **1999**, *33*, (12), 2028-2034.
30. Pereira, J. R.; Mendez, J., Inhibition of Peroxidase by Algal Humic and Fulvic Acids. *Biol Plantarum* **1976**, *18*, (3), 179-182.
 31. Olsson, B.; Ogren, L., Optimization of Peroxidase Immobilization and of the Design of Packed-Bed Enzyme Reactors for Flow-Injection Analysis. *Anal Chim Acta* **1983**, *145*, (Jan), 87-99.
 32. Azevedo, A. M.; Prazeres, D. M. F.; Cabral, J. M. S.; Fonseca, L. P., Stability of Free and Immobilised Peroxidase in Aqueous-Organic Solvents Mixtures. *J Mol Catal B-Enzym* **2001**, *15*, (4-6), 147-153.
 33. Yan, M.; Ge, J.; Liu, Z.; Ouyang, P. K., Encapsulation of Single Enzyme in Nanogel with Enhanced Biocatalytic Activity and Stability. *J Am Chem Soc* **2006**, *128*, (34), 11008-11009.
 34. Wei, W.; Du, J. J.; Li, J.; Yan, M.; Zhu, Q.; Jin, X.; Zhu, X. Y.; Hu, Z. M.; Tang, Y.; Lu, Y. F., Construction of Robust Enzyme Nanocapsules for Effective Organophosphate Decontamination, Detoxification, and Protection. *Adv Mater* **2013**, *25*, (15), 2212-2218.
 35. Chouyyok, W.; Panpranot, J.; Thanachayanant, C.; Prichanont, S., Effects of pH and Pore Characters of Mesoporous Silicas on Horseradish Peroxidase Immobilization. *J Mol Catal B-Enzym* **2009**, *56*, (4), 246-252.
 36. Ravindra, R.; Shuang, Z.; Gies, H.; Winter, R., Protein Encapsulation in Mesoporous Silicate: The Effects of Confinement on Protein Stability, Hydration, and Volumetric Properties. *J Am Chem Soc* **2004**, *126*, (39), 12224-12225.
 37. Feng, W.; Ji, P. J., Enzymes Immobilized on Carbon Nanotubes. *Biotechnol Adv* **2011**, *29*, (6), 889-895.
 38. Zhang, J. L.; Zhang, F.; Yang, H. J.; Huang, X. L.; Liu, H.; Zhang, J. Y.; Guo, S. W., Graphene Oxide as a Matrix for Enzyme Immobilization. *Langmuir* **2010**, *26*, (9), 6083-6085.
 39. Kedersha, N. L.; Heuser, J. E.; Chugani, D. C.; Rome, L. H., Vaults. III. Vault Ribonucleoprotein Particles Open into Flower-Like Structures with Octagonal Symmetry. *J Cell Biol* **1991**, *112*, (2), 225-235.
 40. Mikiyas, Y.; Makabi, M.; Raval-Fernandes, S.; Harrington, L.; Kickhoefer, V. A.; Rome, L. H.; Stewart, P. L., Cryoelectron Microscopy Imaging of Recombinant and Tissue Derived Vaults: Localization of the MVP N Termini and VPARP. *J Mol Biol* **2004**, *344*, (1), 91-105.
 41. Tanaka, H.; Kato, K.; Yamashita, E.; Sumizawa, T.; Zhou, Y.; Yao, M.; Iwasaki, K.; Yoshimura, M.; Tsukihara, T., The Structure of Rat Liver Vault at 3.5 Angstrom Resolution. *Science* **2009**, *323*, (5912), 384-388.
 42. Rome, L. H.; Kickhoefer, V. A., Development of the Vault Particle as a Platform Technology. *ACS Nano* **2013**, *7*, 889-902.
 43. Kedersha, N. L.; Miquel, M. C.; Bittner, D.; Rome, L. H., Vaults. II. Ribonucleoprotein Structures Are Highly Conserved among Higher and Lower Eukaryotes. *J Cell Biol* **1990**, *110*, (4), 895-901.
 44. Hamill, D. R.; Suprenant, K. A., Characterization of the Sea Urchin Major Vault Protein: A Possible Role for Vault Ribonucleoprotein Particles in Nucleocytoplasmic Transport. *Dev Biol* **1997**, *190*, (1), 117-128.

45. Herrmann, C.; Volkandt, W.; Wittich, B.; Kellner, R.; Zimmermann, H., The Major Vault Protein (MVP100) Is Contained in Cholinergic Nerve Terminals of Electric Ray Electric Organ. *Journal of Biological Chemistry* **1996**, *271*, (23), 13908-13915.
46. Vasu, S. K.; Kedersha, N. L.; Rome, L. H., cDNA Cloning and Disruption of the Major Vault Protein Alpha Gene (mvpA) in *Dictyostelium Discoideum*. *Journal of Biological Chemistry* **1993**, *268*, (21), 15356-15360.
47. Vasu, S. K.; Rome, L. H., Dictyostelium Vaults: Disruption of the Major Proteins Reveals Growth and Morphological Defects and Uncovers a New Associated Protein. *Journal of Biological Chemistry* **1995**, *270*, (28), 16588-16594.
48. van Zon, A.; Mossink, M.; Schoester, M.; Scheper, R.; Sonneveld, P.; Wiemer, E., Multiple Human Vault RNAs: Expression and Association with the Vault Complex. *Leukemia* **2001**, *15*, (3), 503-503.
49. Izquierdo, M. A.; Scheffer, G. L.; Flens, M. J.; Shoemaker, R. H.; Rome, L. H.; Scheper, R. J., Relationship of LRP-Human Major Vault Protein to *in vitro* and Clinical Resistance to Anticancer Drugs. *Cytotechnology* **1996**, *19*, (3), 191-197.
50. Casanas, A.; Guerra, P.; Fita, I.; Verdaguer, N., Vault particles: a new generation of delivery nanodevices. *Curr Opin Biotech* **2012**, *23*, (6), 972-977.
51. Champion, C. I.; Kickhoefer, V. A.; Liu, G. C.; Moniz, R. J.; Freed, A. S.; Bergmann, L. L.; Vaccari, D.; Raval-Fernandes, S.; Chan, A. M.; Rome, L. H.; Kelly, K. A., A Vault Nanoparticle Vaccine Induces Protective Mucosal Immunity. *Plos One* **2009**, *4*, (4), e5409.
52. Kedersha, N. L.; Rome, L. H., Isolation and characterization of a novel ribonucleoprotein particle: large structures contain a single species of small RNA. *J. Cell Biol.* **1986**, *103*, (3), 699-709.
53. Kickhoefer, V. A.; Poderycki, M. J.; Chan, E. K. L.; Rome, L. H., The La RNA-Binding Protein Interacts with the Vault RNA and Is a Vault-Associated Protein. *Journal of Biological Chemistry* **2002**, *277*, (43), 41282-41286.
54. Kickhoefer, V. A.; Stephen, A. G.; Harrington, L.; Robinson, M. O.; Rome, L. H., Vaults and Telomerase Share a Common Subunit, TEP1. *The Journal of biological chemistry* **1999**, *274*, (46), 32712-7.
55. Kickhoefer, V. A.; Siva, A. C.; Kedersha, N. L.; Inman, E. M.; Ruland, C.; Streuli, M.; Rome, L. H., The 193-kD Vault Protein, VPARP, Is a Novel Poly(ADP-Ribose) Polymerase. *J Cell Biol* **1999**, *146*, (5), 917-928.
56. Kickhoefer, V. A.; Searles, R. P.; Kedersha, N. L.; Garber, M. E.; Johnson, D. L.; Rome, L. H., Vault Ribonucleoprotein Particles from Rat and Bullfrog Contain a Related Small RNA That Is Transcribed by RNA Polymerase III. *Journal of Biological Chemistry* **1993**, *268*, (11), 7868-7873.
57. Kickhoefer, V. A.; Liu, Y.; Kong, L. B.; Snow, B. E.; Stewart, P. L.; Harrington, L.; Rome, L. H., The Telomerase/Vault-Associated Protein Tep1 Is Required for Vault RNA Stability and Its Association with the Vault Particle. *J Cell Biol* **2001**, *152*, (1), 157-164.
58. Stephen, A. G.; Raval-Fernandes, S.; Huynh, T.; Torres, M.; Kickhoefer, V. A.; Rome, L. H., Assembly of Vault-like Particles in Insect Cells Expressing Only the Major Vault Protein. *Journal of Biological Chemistry* **2001**, *276*, (26), 23217-23220.

59. Han, M.; Kickhoefer, V. A.; Nemerow, G. R.; Rome, L. H., Targeted Vault Nanoparticles Engineered with an Endosomolytic Peptide Deliver Biomolecules to the Cytoplasm. *ACS Nano* **2011**, *5*, 6128-6137.
60. Poderycki, M. J.; Kickhoefer, V. A.; Kaddis, C. S.; Raval-Fernandes, S.; Johansson, E.; Zink, J. I.; Loo, J. A.; Rome, L. H., The Vault Exterior Shell Is a Dynamic Structure that Allows Incorporation of Vault-Associated Proteins into Its Interior. *Biochemistry-Us* **2006**, *45*, (39), 12184-12193.
61. Yang, J. A.; Kickhoefer, V. A.; Ng, B. C.; Gopal, A.; Bentolila, L. A.; John, S.; Tolbert, S. H.; Rome, L. H., Vaults Are Dynamically Unconstrained Cytoplasmic Nanoparticles Capable of Half Vault Exchange. *ACS Nano* **2010**, *4*, (12), 7229-7240.
62. Kickhoefer, V. A.; Garcia, Y.; Mikiyas, Y.; Johansson, E.; Zhou, J. C.; Raval-Fernandes, S.; Minoofar, P.; Zink, J. I.; Dunn, B.; Stewart, P. L.; Rome, L. H., Engineering of Vault Nanocapsules with Enzymatic and Fluorescent Properties. *Proceedings of the National Academy of Sciences of the United States of America* **2005**, *102*, 4348-4352.
63. Buehler, D. C.; Toso, D. B.; Kickhoefer, V. A.; Zhou, Z. H.; Rome, L. H., Vaults Engineered for Hydrophobic Drug Delivery. *Small* **2011**, *7*, 1432-1439.
64. Kar, U. K.; Srivastava, M. K.; Andersson, A.; Baratelli, F.; Huang, M.; Kickhoefer, V. A.; Dubinett, S. M.; Rome, L. H.; Sharma, S., Novel CCL21-Vault Nanocapsule Intratumoral Delivery Inhibits Lung Cancer Growth. *Plos One* **2011**, *6*, (5), e18758.
65. Wang, M.; Abad, D.; Kickhoefer, V. A.; Rome, L. H.; Mahendra, S., Vault Nanoparticles Packaged with Enzymes as an Efficient Pollutant Biodegradation Technology. *ACS Nano* **2015**, *9*, (11), 10931-10940.
66. Mao, L.; Colosi, L. M.; Gao, S. X.; Huang, Q. G., Understanding Ligninase-Mediated Reactions of Endocrine Disrupting Chemicals in Water: Reaction Rates and Quantitative Structure-Activity Relationships. *Environ Sci Technol* **2011**, *45*, (14), 5966-5972.
67. Hofrichter, M., Review: lignin conversion by manganese peroxidase (MnP). *Enzyme Microb Tech* **2002**, *30*, (4), 454-466.
68. Riva, S., Laccases: blue enzymes for green chemistry. *Trends Biotechnol* **2006**, *24*, (5), 219-226.
69. Bourbonnais, R.; Paice, M. G., Oxidation of Nonphenolic Substrates - an Expanded Role for Laccase in Lignin Biodegradation. *Febs Letters* **1990**, *267*, (1), 99-102.
70. Tsai, T. S., Biotreatment of Red Water—A Hazardous Waste Stream from Explosive Manufacture — with Fungal Systems. *Hazardous Waste and Hazardous Materials* **1991**, *8*, (3), 231-244.
71. Khindaria, A.; Grover, T. A.; Aust, S. D., Reductive Dehalogenation of Aliphatic Halocarbons by Lignin Peroxidase of *Phanerochaete chrysosporium*. *Environ Sci Technol* **1995**, *29*, (3), 719-725.
72. Field, J. A.; Jong, E. d.; Costa, G. F.; Bont, J. A. d., Biodegradation of polycyclic aromatic hydrocarbons by new isolates of white rot fungi. *Applied and environmental microbiology* **1992**, *58*, (7), 2219-2226.
73. Wang, C.; Sun, H.; Li, J.; Li, Y.; Zhang, Q., Enzyme activities during degradation of polycyclic aromatic hydrocarbons by white rot fungus *Phanerochaete chrysosporium* in soils. *Chemosphere* **2009**, *77*, (6), 733-738.

74. Huang, X. R.; Wang, D.; Liu, C. X.; Hu, M.; Qu, Y. B.; Gao, P. J., The roles of veratryl alcohol and nonionic surfactant in the oxidation of phenolic compounds by lignin peroxidase. *Biochem Bioph Res Co* **2003**, *311*, (2), 491-494.
75. Wariishi, H.; Valli, K.; Gold, M. H., Oxidative Cleavage of a Phenolic Diarylpropane Lignin Model Dimer by Manganese Peroxidase from Phanerochaete-Chrysosporium. *Biochemistry-Us* **1989**, *28*, (14), 6017-6023.
76. Ollikka, P.; Alhonmaki, K.; Leppanen, V. M.; Glumoff, T.; Rajjola, T.; Suominen, I., Decolorization of Azo, Triphenyl Methane, Heterocyclic, and Polymeric Dyes by Lignin Peroxidase Isoenzymes from Phanerochaete-Chrysosporium. *Applied and environmental microbiology* **1993**, *59*, (12), 4010-4016.
77. Ramírez, D. A.; Muñoz, S. V.; Atehortua, L.; Michel, F. C., Jr., Effects of different wavelengths of light on lignin peroxidase production by the white-rot fungi Phanerochaete chrysosporium grown in submerged cultures. *Bioresource Technology* **2010**, *101*, (23), 9213-9220.
78. Wariishi, H.; Valli, K.; Gold, M. H., Manganese(II) Oxidation by Manganese Peroxidase from the Basidiomycete *Phanerochaete Chrysosporium*. Kinetic Mechanism and Role of Chelators. *Journal of Biological Chemistry* **1992**, *267*, 23688-23695.
79. Guo, M.; Lu, F. P.; Du, L. X.; Pu, J.; Bai, D. Q., Optimization of the expression of a laccase gene from *Trametes versicolor* in *Pichia methanolica*. *Appl Microbiol Biot* **2006**, *71*, (6), 848-852.
80. Tien, M.; Kirk, T. K., Lignin Peroxidase of *Phanerochaete Chrysosporium*. *Method Enzymol* **1988**, *161*, 238-249.
81. Tisma, M.; Znidarsic-Plazl, P.; Vasic-Racki, D.; Zelic, B., Optimization of Laccase Production by *Trametes versicolor* Cultivated on Industrial Waste. *Applied Biochemistry and Biotechnology* **2012**, *166*, (1), 36-46.
82. Johnson, D. R.; Lee, P. K. H.; Holmes, V. F.; Alvarez-Cohen, L., An internal reference technique for accurately quantifying specific mRNAs by real-time PCR with a application to the *tceA* reductive dehalogenase gene. *Applied and environmental microbiology* **2005**, *71*, (7), 3866-3871.
83. O'Callaghan, J.; O'Brien, M. M.; McClean, K.; Dobson, A. D. W., Optimisation of the Expression of a *Trametes versicolor* Laccase Gene in *Pichia pastoris*. *J Ind Microbiol Biot* **2002**, *29*, (2), 55-59.
84. Gu, C. J.; Zheng, F.; Long, L. K.; Wang, J.; Ding, S. J., Engineering the Expression and Characterization of Two Novel Laccase Isoenzymes from *Coprinus comatus* in *Pichia pastoris* by Fusing an Additional Ten Amino Acids Tag at N-Terminus. *Plos One* **2014**, *9*, (4).
85. Jonsson, L. J.; Saloheimo, M.; Penttila, M., Laccase from the white-rot fungus *Trametes versicolor*: cDNA cloning of *lcc1* and expression in *Pichia pastoris*. *Curr Genet* **1997**, *32*, (6), 425-30.
86. Otterbein, L.; Record, E.; Longhi, S.; Asther, M.; Moukha, S., Molecular cloning of the cDNA encoding laccase from *Pycnoporus cinnabarinus* I-937 and expression in *Pichia pastoris*. *Eur J Biochem* **2000**, *267*, (6), 1619-1625.
87. Wada, A.; Saito, Y.; Ohgushi, M., Multiphasic Conformation Transition of Globular-Proteins under Denaturing Perturbation. *Biopolymers* **1983**, *22*, (1), 93-99.

88. Henley, J. P.; Sadana, A., Categorization of Enzyme Deactivations Using a Series-Type Mechanism. *Enzyme Microb Tech* **1985**, *7*, (2), 50-60.
89. Chattopadhyay, K.; Mazumdar, S., Structural and conformational stability of horseradish peroxidase: Effect of temperature and pH. *Biochemistry-Us* **2000**, *39*, (1), 263-270.
90. Urek, R. O.; Pazarlioglu, N. K., Purification and Partial Characterization of Manganese Peroxidase from Immobilized *Phanerochaete Chrysosporium*. *Process Biochem* **2004**, *39*, (12), 2061-2068.
91. Esfandiary, R.; Kickhoefer, V. A.; Rome, L. H.; Joshi, S. B.; Middaugh, C. R., Structural Stability of Vault Particles. *Journal of Pharmaceutical Sciences* **2009**, *98*, 1376-1386.
92. Sheremata, T. W.; Hawari, J., Mineralization of RDX by the white rot fungus *Phanerochaete chrysosporium* to carbon dioxide and nitrous oxide. *Environ Sci Technol* **2000**, *34*, (16), 3384-3388.
93. Hirano, T.; Honda, Y.; Watanabe, T.; Kuwahara, M., Degradation of Bisphenol A by the Lignin-Degrading Enzyme, Manganese Peroxidase, Produced by the White-Rot Basidiomycete, *Pleurotus Ostreatus*. *Biosci Biotech Bioch* **2000**, *64*, (9), 1958-1962.
94. Kedersha, N. L.; Rome, L. H., Vaults - Large Cytoplasmic Rnps That Associate with Cytoskeletal Elements. *Mol Biol Rep* **1990**, *14*, (2-3), 121-122.
95. Kickhoefer, V. A.; Vasu, S. K.; Rome, L. H., Vaults are the answer, what is the question? *Trends Cell Biol* **1996**, *6*, (5), 174-178.

Appendices

1 ATGGCCTTCAAGCAGCTCTTCGCAGCTATCTCTCTCGCTCTCTCGCTCTCGGCTGCGAAC 60
1 M A F K Q L F A A I S L A L S L S A A N 20
61 GCGGCTGCGGTTATCGAGAAGCGCGCCACCTGTTCCAACGGCAAGACCGTTCGGCGATGCG 120
21 A A A V I E K R A T C S N G K T V G D A 40
121 TCGTGCTGCGCTTGGTTTCGACGTCCTGGATGATATCCAGCAGAACCTGTTCCACGGCGGC 180
41 S C C A W F D V L D D I Q Q N L F H G G 60
181 CAGTGCGGGCGCTGAGGCGCACGAGTCGATTCTCGTCTTCCACGACTCCATCGCAATT 240
61 Q C G A E A H E S I R L V F H D S I A I 80
241 TCGCCCGCCATGGAGGCACAGGGCAAGTTCGGCGGCGGTGGTGCTGACGGCTCCATCATG 300
81 S P A M E A Q G K F G G G G A D G S I M 100
301 ATCTTCGACGATATCGAGACTGCGTTCACCCTAACATCGGTCTCGACGAGATCGTCAAG 360
101 I F D D I E T A F H P N I G L D E I V K 120
361 CTCCAGAAGCCATTTCGTTTCAGAAGCACGGTGTACCCCTGGTGACTTCATCGCCTTCGCT 420
121 L Q K P F V Q K H G V T P G D F I A F A 140
421 GGTGCTGTGCGCTCAGCAACTGCCCTGGTGCCCCGAGATGAACTTCTTCACTGGTCGT 480
141 G A V A L S N C P G A P Q M N F F T G R 160
481 GCACCTGCTACCCAGCCCCGCTCCTGATGGCCTTGTCCCCGAGCCCTTCCACACTGTCGAC 540
161 A P A T Q P A P D G L V P E P F H T V D 180
541 CAAATCATCAACCGTGTCAACGACGCAGGCGAGTTCGATGAGCTCGAGCTTGTCTGGATG 600
181 Q I I N R V N D A G E F D E L E L V W M 200
601 CTCTCCGCGCACTCCGTGCGAGCGGTGAACGACGTCGACCCGACCGTCCAGGGTCTGCC 660
201 L S A H S V A A V N D V D P T V Q G L P 220
661 TTTGACTCGACCCCCGGAATCTTCGACTCCCAGTTCTTCGTCGAGACTCAGCTTCGTGGT 720
221 F D S T P G I F D S Q F F V E T Q L R G 240
721 ACCGCTTCCCCGGCTCTGGCGGCAACCAAGGCGAGGTCGAGTCGCCGCTCCCTGGCGAA 780
241 T A F P G S G G N Q G E V E S P L P G E 260
781 ATTGCATCCAGTCCGACCACACTATCGCCCGGACTCACGCACGGCGTGTGAATGGCAG 840
261 I R I Q S D H T I A R D S R T A C E W Q 280
841 TCCTTCGTCAACAACAGTCCAAGCTCGTCGATGACTTCCAATTCATTTTCTCGCCCTC 900
281 S F V N N Q S K L V D D F Q F I F L A L 300
901 ACCCAGCTCGGCCAGGACCCGAACGCGATGACCGACTGCTCGGATGTTATCCCGCAGTCC 960
301 T Q L G Q D P N A M T D C S D V I P Q S 320
961 AAGCCCATCCCTGGCAACCTCCCATTCTCGTTCTTCCCCGCTGGCAAGACCATCAAAGAC 1020
321 K P I P G N L P F S F F P A G K T I K D 340
1021 CTTCAGCAGCCCTCTCCCGACAGCCCGCTTCCCGACTCTCAGCAGCTCTCCCGCCCGCCAC 1080

```
1081   ACGTCCGTCCAGCGCATCCCTCCGCCTCCGGGTGCTTAA   1119
361     T S V Q R I P P P P G A END           372
```

Figure S1. Complete Nucleotide Sequence of Lignin Peroxidase from *P. chrysosporium*. Isolated LiP gene is 1119 bp long, coding for 372 amino acids, which are shown below the nucleotide sequence. Primers binding sites are marked with shading. Following initial codon, a leader sequence (amino acids 1-28) predominantly containing hydrophobic amino acids is underlined.

1 ATGGCCTTCGGTTCTCTCCTCGCCTTCGTGGCTCTCGCCGCCATAACTCGCGCCGCCCG 60
1 M A F G S L L A F V A L A A I T R A A P 20

61 ACTGCGGAGTCTGCAGTCTGTCCAGACGGTACCCGCGTCACCAACGCGGCGTGTGCGCT 120
21 T A E S A V C P D G T R V T N A A C C A 40

121 TTCATTCCGCTCGCACAGGATTTGCAAGAGACTCTGTTCCAGGGTGACTGTGGCGAAGAT 180
41 F I P L A Q D L Q E T L F Q G D C G E D 60

181 GCCCACGAAGTCATCCGTCTGACCTTCCACGACGCTATTGCAATCTCCCAGAGCCTAGGT 240
61 A H E V I R L T F H D A I A I S Q S L G 80

241 CCTCAGGCTGGCGGCGGTGCTGACGGCTCCATGCTGCACTTCCCACAAATCGAGCCCAAC 300
81 P Q A G G G A D G S M L H F P T I E P N 100

301 TTCTCCGCCAACAGCGGCATCGATGACTCCGTCAACAACCTTGCTTCCCTTCATGCAGAAA 360
101 F S A N S G I D D S V N N L L P F M Q K 120

361 CACGACACCATCAGTGCCGCCGATCTTGTACAGTTGCGCGGTGCGGTGCGCTGAGCAAC 420
121 H D T I S A A D L V Q F A G A V A L S N 140

421 TGCCAGGTGCTCCTCGCCTCGAGTTCATGGCTGGACGTCCGAACACTACCATCCCCGCA 480
141 C P G A P R L E F M A G R P N T T I P A 160

481 GTTGAGGGCCTCATTCTGAGCCTCAAGACAGCGTCACCAAATCCTGCAGCGCTTCGAG 540
161 V E G L I P E P Q D S V T K I L Q R F E 180

541 GACGCCGGCAACTTCTCGCCGTTTCGAGGTGCTCTCGCTCCTGGCTTCACACACCGTTGCT 600
181 D A G N F S P F E V V S L L A S H T V A 200

601 CGTGCGGACAAGGTCGACGAGACCATCGATGCTGCGCCCTTCGACTCGACACCCTTCACC 660
201 R A D K V D E T I D A A P F D S T P F T 220

661 TTCGACACCCAGGTGTTCTCGAGGTCTGCTCAAGGGCACAGGCTTCCCGGGCTCGAAC 720
221 F D T Q V F L E V L L K G T G F P G S N 240

721 AACAAACCCGGCGAGGTGATGTCGCCGCTCCCACTCGGCAGCGGCAGCGACACGGGCGAG 780
241 N N T G E V M S P L P L G S G S D T G E 260

781 ATGCGCCTGCAGTCCGACTTTGCGCTCGCGCGGACGAGCGCACGGCGTCTTCTGGCAG 840
261 M R L Q S D F A L A R D E R T A C F W Q 280

841 TCGTTCGTCAACGAGCAGGAGTTCATGGCGGCGAGCTTCAAGGCCGCGATGGCGAAGCTT 900
281 S F V N E Q E F M A A S F K A A M A K L 300

901 GCGATCCTCGGCCACAGCCGAGCAGCCTCATTGACTGCAGCGACGTCGTCCCCGTCCCG 960
301 A I L G H S R S S L I D C S D V V P V P 320

961 AAGCCCCCGTCAACAAGCCCGGACGTTCCCCGCGACGAAGGGCCCCAAGGACCTCGAC 1020
321 K P A V N K P A T F P A T K G P K D L D 340

1021 ACGCTCACGTGCAAGGCCCTCAAGTTCGCGACGCTGACCTCTGACCCCGGTGCTACCGAG 1080
341 T L T C K A L K F P T L T S D P G A T E 360

```

1081  ACCCTCATCCCCCACTGCTCCAACGGCGGCATGTCCTGCCCTGGTGTTCAGTTCGATGGC 1140
361   T L I P H C S N G G M S C P G V Q F D G 380

1141  CCTGCCTAA 1149
381   P A END 382

```

Figure S2. Complete Nucleotide Sequence of Manganese Peroxidase from *P. chrysosporium*. Isolated MnP gene is 1149 bp long, coding for 382 amino acids, which are shown below the nucleotide sequence. Primers binding sites are marked with shading. Following initial codon, a leader sequence (amino acids 1-24) predominantly containing hydrophobic amino acids is underlined.

1 ATGTCGAGGTTTTCACTCTCTTCTCGCTTTTCGTCGTTGCTTCCCTTACGGCTGTGGCCCAC 60
1 M S R F H S L L A F V V A S L T A V A H 20

61 GCTGGTATCGGTCCCGTCGCCGACCTAACCATCACCAACGCAGCGGTGAGCCCCGACGGG 120
21 A G I G P V A D L T I T N A A V S P D G
40

121 TTTTCTCGCCAGGCCGTCGTCGTGAACGGCGGCACCCCTGGCCCTCTCATCACGGGTAAC 180
41 F S R Q A V V V N G G T P G P L I T G N 60

181 ATGGGGGATCGCTTCCAGCTCAATGTCATCGACAACCTTACCAACCACACGATGCTGAAG 240
61 M G D R F Q L N V I D N L T N H T M L K 80

241 AGCACGAGTATTCCTGACGCGTTTCTTCCAGAAGGGCACCAACTGGGCCGACGGTCCC 300
81 S T S I H W H G F F Q K G T N W A D G P 100

301 GCCTTCATCAACCAGTGCCCGATCTCATCTGGTCACTCGTTCCCTGTACGACTTCCAGGTT 360
101 A F I N Q C P I S S G H S F L Y D F Q V 120

361 CCTGACCAGGCTGGTACCTTCTGGTATCACAGTCACTTGTCTACGCAGTACTGTGATGGT 420
121 P D Q A G T F W Y H S H L S T Q Y C D G 140

421 TTGAGGGGTCCGTTTCGTTGTTTACGACCCGAATGACCCGGCCGCCGACCTGTACGACGTC 480
141 L R G P F V V Y D P N D P A A D L Y D V 160

481 GACAACGACGACACTGTCATTACCCTTGTGGATTGGTACCACGTCGCCCGGAAGCTGGGC 540
161 D N D D T V I T L V D W Y H V A A K L G 180

541 CCCGCATTCCCTCTCGGCGCCGACGCCACCCTCATCAACGGTAAGGGACGCTCCCCCAGC 600
181 P A F P L G A D A T L I N G K G R S P S 200

601 ACGACCACCGCGGACCTCTCAGTTATCAGCGTCACCCCGGGTAAACGCTACCGTTTCCGC 660
201 T T T A D L S V I S V T P G K R Y R F R 220

661 CTGGTGTCCCTGTCGTGCGACCCCAACTACAGTTTACGATCGATGGTCAACAATGACG 720
221 L V S L S C D P N Y T F S I D G H N M T 240

721 ATCATCGAGACCGACTCAATCAACACGGCGCCCTCGTCGTCGACTCCATTGATCTTTC 780
241 I I E T D S I N T A P L V V D S I Q I F 260

781 GCCGCCCAGCGTTACTCCTTCGTGCTCGAGGCCAACCAGGCCGTCGACAACACTACTGGATT 840
261 A A Q R Y S F V L E A N Q A V D N Y W I 280

841 CGCGCCAACCCGAACCTTCGGTAACGTCGGGTTACCCGGCGGCATTAACCTCGGCTATCCTC 900
281 R A N P N F G N V G F T G G I N S A I L 300

901 CGCTACGATGGTGCCGCTGCCGTGGAGCCCACCACCACGCAAACCACGTCGACTGCGCCG 960
301 R Y D G A A A V E P T T T Q T T S T A P 320

961 CTCAACGAGGTCAACCTGCACCCGCTGGTTGCCACCGCTGTGCCTGGCTCGCCCGTCGCT 1020
321 L N E V N L H P L V A T A V P G S P V A 340

1021 GGTGGTGTGACCTGGCCATCAACATGGCGTTCAACTTCAACGGCACCAACTTCTTCATC 1080
341 G G V D L A I N M A F N F N G T N F F I 360

```

1081 AACGGCGCGTCTTTACGCCCCGACCGTGCCTGTCCTCCTCCAGATCATCAGCGGCGCG 1140
361 N G A S F T P P T V P V L L Q I I S G A 380

1141 CAGAACGCGCAGGACCTCCTGCCCTCCGGCAGCGTCTACTCGCTTCCCTCGAACGCCGAC 1200
381 Q N A Q D L L P S G S V Y S L P S N A D 400

1201 ATCGAGATCTCCTTCCCCGCGACCGCCGCCGCCCGGGTGCGCCCCACCCCTTCCACTTG 1260
401 I E I S F P A T A A A P G A P H P F H L 420

1261 CACGGGCACGCGTTTCGCGGTCGTCCGCAGCGCCGGCAGCACGGTTTACAACACTACGACAAC 1320
421 H G H A F A V V R S A G S T V Y N Y D N 440

1321 CCTATCTTCCGCGACGTCGTGTCAGCACGGGGACGCCTGCGGCCGGTGACAACGTCACGATC 1380
441 P I F R D V V S T G T P A A G D N V T I 460

1381 CGCTTCCGCACCGACAACCCCGGCCCGTGGTTCCTCCACTGCCACATCGACTTCCACCTC 1440
461 R F R T D N P G P W F L H C H I D F H L 480

1441 GAGGCCGGCTTCGCCGTCGTGTTTCGCGGAGGACATCCCCGACGTCGCGTCGGCGAACCCC 1500
481 E A G F A V V F A E D I P D V A S A N P 500

1501 GTCCCCAGGCGTGGTCCGACCTCTGCCCGACCTACGACGCGCGCGACCCCGAGCGACCAG 1560
501 V P Q A W S D L C P T Y D G A T R A T S 520

1561 TAA
521 END

```

Figure S3. Complete Nucleotide Sequence of Laccase from *T. versicolor*. Isolated laccase gene is 1563 bp long, coding for 520 amino acids, which are shown below the nucleotide sequence. Primers binding sites are marked with shading. Following initial codon, a leader sequence (amino acids 1-21) predominantly containing hydrophobic amino acids is underlined.

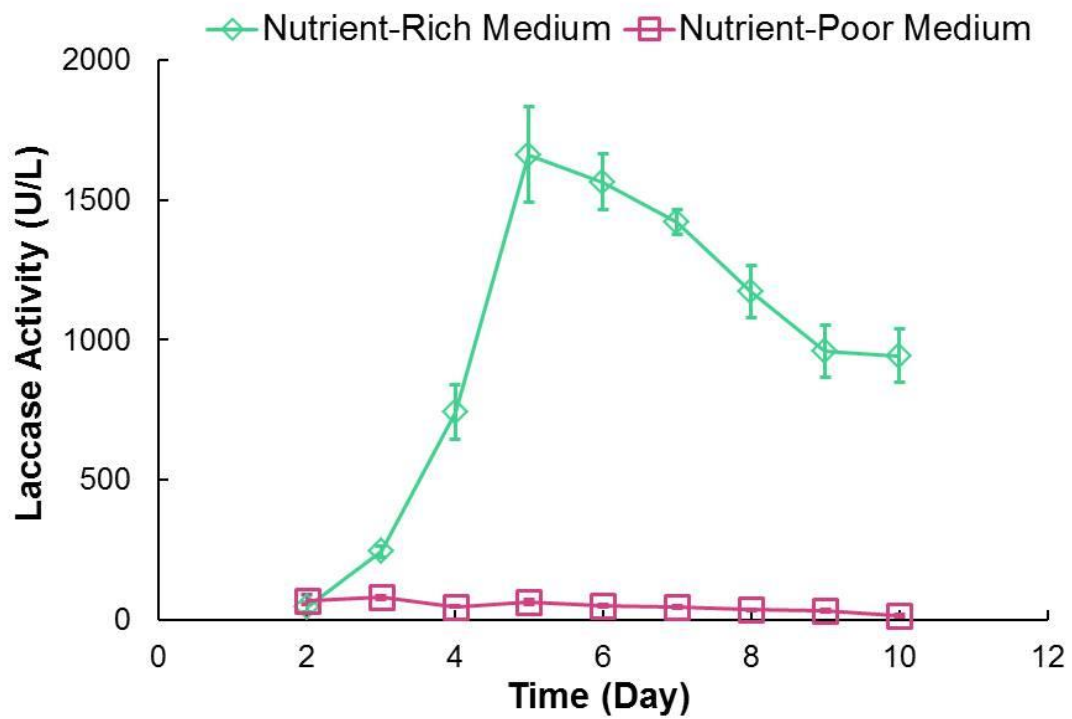


Figure S4. Production of Laccase Enzyme by *T. versicolor* in Two Growth Media.